

Linking bifurcation analysis of Holling–Tanner model with generalist predator to a changing environment

Chuang Xiang¹ | Jicai Huang¹ | Hao Wang² 

¹ School of Mathematics and Statistics,
Central China Normal University,
Wuhan, Hubei, China

² Department of Mathematical and
Statistical Sciences, University of Alberta,
Edmonton, Alberta, Canada

Correspondence

Jicai Huang, School of Mathematics and
Statistics, Central China Normal
University, Wuhan, Hubei 430079, P. R.
China.

Email: hjc@mail.ccnu.edu.cn

Hao Wang, Department of Mathematical
and Statistical Sciences, University of
Alberta, Edmonton, Alberta T6G 2G1,
Canada. Email: hao8@ualberta.ca

Funding information

National Natural Science Foundation of
China; Natural Sciences and Engineering
Research Council of Canada

Abstract

Bifurcation theory has been highly popular in the analysis of mathematical models. However, stability and bifurcation analyses are only for asymptotic dynamics while applied scientists care more about transient dynamics. In this paper, we first rigorously analyze Holling–Tanner model with generalist predators who have alternative food sources, and then discuss transient dynamics via a changing environment. For a constant environment, we provide a complete bifurcation analysis with high codimension. It is shown that the highest codimension of a nilpotent cusp is 3, and the model can undergo degenerate Bogdanov–Takens bifurcation of codimension 3. Moreover, by using resultant elimination to solve the semialgebraic varieties of Lyapunov coefficients, we show that a center-type equilibrium is a weak focus with order at most 2, and the model can exhibit Hopf bifurcation of codimension 2. Our results indicate that generalist predators can cause not only richer dynamics and bifurcations, but also the extinction of prey for some positive initial densities. Numerical simulations, including the coexistence of a limit cycle and a homoclinic cycle, tristability, two limit cycles, are presented to illustrate the theoretical results. In a changing environment, the populations start along one stable

state but can track unstable states or oscillations when the system crosses a bifurcation point, and then tend to another stable state or oscillations. This tracking on transient dynamics predicts regime shifts under environmental changes. When environmental conditions vary, the populations can track unstable states in the constant environment. The rate of environmental change determines how long the system tracks an unstable state although finally the solution under environmental change is attracted to a stable steady state or limit cycle. Finally, we focus on a periodic environment and find that the populations converge to a periodic solution or an invariant torus depending on both the initial environmental capacity and the amplitude of periodic fluctuation.

KEYWORDS

degenerate Bogdanov–Takens bifurcation, environmental change, generalist predator, Holling–Tanner model, Hopf bifurcation, persistence, resultant elimination, regime shifts, transient dynamics

1 | INTRODUCTION

Bifurcation theory has been widely applied in analyzing mathematical models to show the change of asymptotic dynamics according to key parameters. The resulting insights can be useful for long-term predictions. However, scientists are more interested in transient dynamics which may or may not be linked to asymptotic dynamics. Here, we first introduce and rigorously perform stability and bifurcation analysis for the general Leslie type predator–prey system and then link the mathematical findings to transient dynamics under environmental changes. Environmental changes such as global warming have received much attention in the past two decades, hence to understand the impact of that on an ecosystem is appealing.

To introduce the mathematical model, let $x(t)$ and $y(t)$ denote densities of the prey and predators at time t , respectively. The general Leslie type predator–prey system takes the following form (Freedman and Mathsen,¹ Hsu and Huang²):

$$\begin{aligned}\dot{x} &= rx\left(1 - \frac{x}{K}\right) - p(x)y, \\ \dot{y} &= sy\left(1 - \frac{y}{hx}\right),\end{aligned}\tag{1}$$

where r and K describe the intrinsic growth rate and the carrying capacity of the prey, respectively; $p(x)$ is the functional response of predators to their prey density, which refers to the change in the density of prey per unit time per predator as the prey density changes.

System (1) is different from the classical Gause type predator–prey system and its generalized version.^{3,4} In (1), the predator grows logistically with intrinsic growth rate s and environmental carrying capacity proportional to the size of prey available (Leslie,⁵ May⁶), that is, hx with h a measure of the food quality. The term $\frac{y}{hx}$ is called Leslie–Gower term.⁷

System (1) with different functional responses $p(x)$ have been studied extensively, see, for example, Leslie and Gower,⁷ Hsu and Huang² for Lotka–Volterra type, May,⁶ Tanner,⁸ Collings,⁹ Hsu and Huang,^{2,10,11} Gasull et al,¹² Sáez and González-Olivares,¹³ Braza¹⁴ for Holling type II, Liang and Pan¹⁵ for ratio-dependent type, Hsu and Huang² for Holling type III, Huang et al,¹⁶ Dai et al,¹⁷ Wang and Zhang¹⁸ for generalized Holling type III, Li and Xiao,¹⁹ Huang et al,²⁰ Zhang and Su²¹ for simplified Holling type IV, and so forth. Comparing Leslie-type predator–prey system (1) with corresponding Gause-type system under the same $p(x)$, we conclude that system (1) can undergo richer dynamical behaviors and bifurcation phenomena.

When $p(x)$ takes the most widely used Holling type II functional response $\frac{mx}{n+x}$, system (1) becomes as the Holling–Tanner model (^{6,8,22})

$$\begin{aligned}\dot{x} &= rx\left(1 - \frac{x}{K}\right) - \frac{mxy}{n+x}, \\ \dot{y} &= sy\left(1 - \frac{y}{hx}\right),\end{aligned}\tag{2}$$

where m is the maximum rate of predation, and n is called the half-saturation constant. There have been extensive studies about model (2),^{2,9–14} such as the existence of a unique positive equilibrium and two limit cycles, the uniqueness of limit cycle, Hopf bifurcation of codimension 1 and 2, especially the local stability of the unique positive equilibrium does not imply its global stability. Moreover, by the asymptotic dynamics at $(0,0)$ in the interior of the first quadrant and the boundary dynamics,^{12,13} it is worth to noting that both predator and prey populations with positive initial values will persist forever for model (2).

In (1) and (2), the predator is a *specialist predator*, which relies on a single prey species to survive and will die out in absence of this prey. While some predators are *generalist predators*, which have several alternative prey species for food and can persist by switching to other food sources even when one particular prey species is scarce. In the real world, these two kinds of predation play an important role in the interaction and distribution of some species, such as it has been proposed that specialist predators (like small mustelids) maintain the regular multiannual cycles of rodent populations in northern Fennoscandia. Generalist predators (like foxes, common buzzards, cats, etc.) are assumed to stabilize rodent populations in southern Fennoscandia.²³ There are a large number of studies about predator–prey models with specialist predator, while very few authors considered the effect of generalist predation on predator–prey models, even in simple two-species models.²⁴ There are different methods to consider generalist predation in classical Gause-type models, such as: (i) suppose that alternative resources are constant and add a directly density-dependent mortality to the prey's equation^{23,25,26}; (ii) suppose that alternative resources are constant and the predator's equation is logistic or logistic-like form in the absence of the prey^{24,27–29}; and (iii) suppose that alternative resources are not constant and consider high-dimensional models, such as two prey and one predator species.³⁰

Based on Holling–Tanner model (2), Aziz-Alaoui and Daher Okiye³¹ proposed the modified Holling–Tanner model considering alternative food sources for predators:

$$\begin{aligned}\dot{x} &= rx\left(1 - \frac{x}{K}\right) - \frac{mxy}{n+x}, \\ \dot{y} &= sy\left(1 - \frac{y}{hx+K_2}\right),\end{aligned}\tag{3}$$

where $hx + K_2$ is the new carrying capacity for predators, and $K_2 > 0$ can be seen as an extra constant carrying capacity coming from all other food sources for predators. When $x = 0$, the predator equation in (3) becomes $\dot{y} = sy\left(1 - \frac{y}{K_2}\right)$, that is, a logistic growth equation, which means that predators can survive by switching to other food sources even when one particular prey species is terribly scarce. Thus, the predator in (3) can be seen as a generalist predator. Model (3) and its variations have been extensively studied. When (3) has a unique positive equilibrium and is elementary, Aziz-Alaoui and Daher Okiye³¹ provided some sufficient conditions to assure its global stability. In Ref. 32, when the parameters are positive and T-periodic, some sufficient conditions were obtained for the existence of global attractive positive periodic solutions by using a coincidence degree theorem and constructing a suitable Lyapunov function. In a preprint, using Dulac's criterion and Liapunov function, Li and Song³³ gave a very detailed study about the global stability of a unique positive equilibrium, which improves the known results. Wang and Zhang¹⁸ studied the existence and uniqueness of a relaxation oscillation in (3) with slow-fast two time scale by using geometric singular perturbation theory. Finally, in Ref. 34, Giné and Valls explored the existence of nonlinear oscillations in (3), they proved that at least one limit cycle can bifurcate from one positive equilibrium but it is never a center.

The response of populations to environmental fluctuations has been and remains a cutting-edge area of ecological research. Linking transient dynamics under a changing environment to stable and unstable states in the constant environment would be insightful in uncovering the underlying mechanisms. To describe the rate of environmental change in habitat quality, Arumugam et al³⁵ assumed that the prey's carrying capacity is a linear function of time t . Based on model (3) and Ref. 35, we formulate the following model in a changing environment:

$$\begin{aligned}\dot{x} &= rx\left(1 - \frac{x}{K}\right) - \frac{mxy}{n+x}, \\ \dot{y} &= sy\left(1 - \frac{y}{hx+K_2}\right), \\ \dot{K} &= \mu,\end{aligned}\tag{4}$$

where μ is the rate of environmental change in habitat quality (carrying capacity). From the third equation of system (4), we have $K(t) = K_0 + \mu t$ (K_0 is the initial value), which represents the possible directional environmental change.

In a constant environment (i.e., $\mu = 0$), system (4) becomes system (3). Although plentiful qualitative results about global stability and the existence of limit cycle have been revealed for system (3), the nonlinear dynamics and complex bifurcation phenomena of system (3) are not well understood. Especially, the complete analysis on bifurcations with high codimension still remain untouched, we list them in the following:

- (i) **Nilpotent bifurcation with high codimension:** System (3) has at most two positive equilibria, they can coalesce into a unique one, which is degenerate and may be a nilpotent equilibrium, then what is its exact type and final codimension? Whether system (3) can undergo corresponding nilpotent bifurcation with corresponding codimension or not?
- (ii) **Hopf bifurcation with high codimension:** When system (3) has a center-type equilibrium, is it a center or focus? If it is a focus, then what is its highest order? Whether system (3) can undergo Hopf bifurcation with highest codimension or not?

In this paper, for the first problem above, by using center manifold theorem and normal form theory, we will show that the nilpotent equilibrium is a cusp with codimension at most 3, and system (3) can undergo degenerate Bogdanov–Takens bifurcation of codimension 3, the cusp of codimension 3 can be seen as the organizing center of the bifurcation set. For the second problem, by using some algebraic methods, including resultant elimination in Ref. 36 and Complete Discrimination System for polynomials in Yang,³⁷ to solve the semialgebraic varieties of Lyapunov coefficients (or focal values), we will show that the center-type equilibrium is a weak focus with order at most 2, and the system can exhibit Hopf bifurcation of codimension 2. Finally, numerical simulations, including the coexistence of a limit cycle and a homoclinic cycle, two limit cycles enclosing a stable equilibrium, are presented to illustrate the theoretical results.

In a changing environment (i.e., $\mu \neq 0$), we will study the effect of the rate of change in carrying capacity on the dynamics in system (4), compare dynamics in the changing environment with those obtained by bifurcation analysis for the corresponding constant environment, and predict the long-term dynamics and persistence of ecological systems under continuous environmental change. We further explore the impact of a periodic environment on dynamics.

The remaining paper is organized as follows. In Section 2, we study the equilibria and their types of system (3), and then discuss bifurcations with high codimension, including Hopf bifurcation with codimension up to 2 and degenerate Bogdanov–Takens bifurcation of codimension 3, in system (3). In Section 3, we explore the impact of environmental change on the dynamics in system (4). Finally, we discuss our results in Section 4.

2 | CONSTANT ENVIRONMENT

Under constant environment $\mu = 0$, we will give a complete analysis on bifurcations with high codimension for system (4).

Before going into details, we make the following scaling:

$$x = K\bar{x}, \quad y = hK\bar{y}, \quad t = \frac{\tau}{r}, \quad (5)$$

then system (3) becomes (drop the bar and still denote τ by t)

$$\begin{aligned} \dot{x} &= x(1-x) - \frac{axy}{x+k_1}, \\ \dot{y} &= cy \left(1 - \frac{y}{x+k_2} \right), \end{aligned} \quad (6)$$

where

$$a = \frac{mh}{r}, \quad c = \frac{s}{r}, \quad k_1 = \frac{n}{K}, \quad k_2 = \frac{K_2}{hK}, \quad (7)$$

and they are all positive. We consider system (6) in $\mathbb{R}_+^2 = \{(x, y) | x \geq 0, y \geq 0\}$ in the biological perspective.

2.1 | Equilibria and their types

In this section, we analyze the type of nonnegative equilibria of system (6). The positive invariant and bounded region of system (6) is

$$\Omega = \{(x, y) | 0 \leq x \leq 1, 0 \leq y \leq k_2 + 1\}. \quad (8)$$

The Jacobian matrix of system (6) at any equilibrium $E(x, y)$ takes the form

$$J(E) = \begin{pmatrix} 1 - 2x - \frac{ak_1y}{(k_1+x)^2} & -\frac{ax}{k_1+x} \\ \frac{cy^2}{(k_2+x)^2} & c - \frac{2cy}{(k_2+x)} \end{pmatrix}, \quad (9)$$

and

$$\begin{aligned} \text{Det}(J(E)) &= \left(1 - 2x - \frac{ak_1y}{(x+k_1)^2}\right) \left(c - \frac{2cy}{x+k_2}\right) + \frac{acxy^2}{(x+k_1)(x+k_2)^2}, \\ \text{Tr}(J(E)) &= 1 + c - 2x - \frac{ak_1y}{(x+k_1)^2} - \frac{2cy}{x+k_2}. \end{aligned} \quad (10)$$

2.1.1 | Boundary equilibria and their types

System (6) always has three boundary equilibria $E_{00}(0, 0)$, $E_{10}(1, 0)$, and $E_{20}(0, k_2)$.

Lemma 1. *System (6) always has three boundary equilibria $E_{00}(0, 0)$, $E_{10}(1, 0)$, and $E_{20}(0, k_2)$. E_{00} is always a hyperbolic unstable node, E_{10} is always a hyperbolic saddle. E_{20} is a hyperbolic saddle if $k_2 < \frac{k_1}{a}$, a hyperbolic stable node if $k_2 > \frac{k_1}{a}$ and a degenerate equilibrium if $k_2 = \frac{k_1}{a}$.*

Theorem 1. *When $k_2 = \frac{k_1}{a}$, E_{20} is a degenerate equilibrium. Moreover,*

- (I) *if $k_1 \neq 1 - a$, then E_{20} is a saddle-node of codimension 1, which includes a stable parabolic sector in the right (or left) half plane when $k_1 > 1 - a$ (or $k_1 < 1 - a$, $a < 1$);*
- (II) *if $k_1 = 1 - a$ and $a < 1$, then E_{20} is a stable degenerate node of codimension 2.*

Proof. We make the following transformations successively:

$$\begin{aligned} x &= x_1, & y &= y_1 + k_2; \\ x_1 &= x_2, & y_1 &= x_2 + y_2, & t &= -\frac{\tau}{c}, \end{aligned} \tag{11}$$

then system (6) becomes as (still denote τ by t)

$$\begin{aligned} \dot{x}_2 &= -\frac{1-a-k_1}{ck_1}x_2^2 + \frac{a}{ck_1}x_2y_2 + \frac{1-a}{ck_1^2}x_2^3 - \frac{a}{ck_1^2}x_2^2y_2 + o(|x_2, y_2|^3), \\ \dot{y}_2 &= y_2 + \frac{1-a-k_1}{ck_1}x_2^2 - \frac{a}{ck_1}x_2y_2 + \frac{a}{k_1}y_2^2 - \frac{1-a}{ck_1^2}x_2^3 + \frac{a}{ck_1^2}x_2^2y_2 - \frac{a^2}{k_2^2}x_2y_2^2 + o(|x_2, y_2|^3), \end{aligned} \tag{12}$$

and according to Theorem 7.1 in chapter 2 of Zhang et al,³⁸ E_{20} is a saddle-node, which includes a stable parabolic sector in the right (or left) half plane of \mathbb{R}^2 if $k_1 > 1 - a$ (or $k_1 < 1 - a$ and $a < 1$).

If $k_1 = 1 - a$ and $a < 1$, then the coefficient of x_2^2 term in the first equation of system (12) is equal to zero. According to center manifold theorem, we suppose that $y_2 = m_1x_2^2 + m_2x_2^3 + o(|x_2|^3)$, and substitute it to $\dot{y}_2 = 0$, then we have

$$m_1 = 0, \quad m_2 = \frac{1}{c(1-a)}. \tag{13}$$

Substituting $y_2 = \frac{1}{c(1-a)}x_2^3 + o(|x_2|^3)$ into the first equation of system (12), we can get the reduced system restricted to the center manifold

$$\dot{x}_2 = \frac{1}{c(1-a)}x_2^3 + o(|x_2|^3), \tag{14}$$

again by Theorem 7.1 in chapter 2 of Zhang et al,³⁸ E_{20} is a stable degenerate node. ■

2.1.2 | Positive equilibria and their types

Now we study the positive equilibria of system (6). The positive equilibrium $E(x, y)$ must satisfy

$$\begin{aligned} 1 - x - \frac{ay}{k_1 + x} &= 0, \\ 1 - \frac{y}{k_2 + x} &= 0, \end{aligned} \tag{15}$$

from which we get that x is a root of the equation

$$x^2 - (1 - a - k_1)x + ak_2 - k_1 = 0, \tag{16}$$

in the interval $(0,1)$. The second-order algebraic equation (16) can have one, or two positive roots in the interval $(0,1)$, which means system (6) can have one, or two positive equilibria.

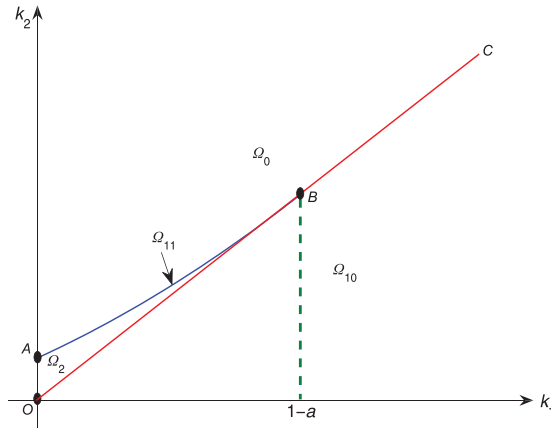


FIGURE 1 Positive equilibria distribution in $(k_1 - k_2)$ plane when $0 < a < 1$. Blue curve \widehat{AB} : $k_2 = \frac{(1-a-k_1)^2 + 4k_1}{4a}$, $0 < k_1 < 1 - a$. Red line: $k_2 = \frac{k_1}{a}$. Green line: $k_1 = 1 - a$

Let

$$F(x) = x^2 - (1 - a - k_1)x + ak_2 - k_1, \quad (17)$$

$$F'(x) = \frac{dF(x)}{dx} = 2x - (1 - a - k_1).$$

By some calculations, we can know that $\text{Det}(J(\bar{E}))$ and $F'(\bar{x})$ satisfy the following relation:

$$\text{Det}(J(\bar{E})) = \frac{c\bar{x}}{k_1 + \bar{x}} F'(\bar{x}). \quad (18)$$

According to the number of positive equilibria of (6), we can classify the parameters space into the following four regions (see Figure 1):

$$\begin{aligned} \Omega_0 &:= \left\{ (a, k_1, k_2) \in \mathbb{R}_+^3 \mid k_2 > \frac{(1-a-k_1)^2 + 4k_1}{4a} \text{ and } k_1 < 1-a, \text{ or } k_2 \geq \frac{k_1}{a} \text{ and } k_1 \geq 1-a \right\}, \\ \Omega_{10} &:= \left\{ (a, k_1, k_2) \in \mathbb{R}_+^3 \mid k_2 < \frac{k_1}{a}, \text{ or } k_2 = \frac{k_1}{a}, k_1 < 1-a \text{ and } a < 1 \right\}, \\ \Omega_{11} &:= \left\{ (a, k_1, k_2) \in \mathbb{R}_+^3 \mid k_2 = \frac{(1-a-k_1)^2 + 4k_1}{4a}, k_1 < 1-a, a < 1 \right\}, \\ \Omega_2 &:= \left\{ (a, k_1, k_2) \in \mathbb{R}_+^3 \mid \frac{k_1}{a} < k_2 < \frac{(1-a-k_1)^2 + 4k_1}{4a}, k_1 < 1-a, a < 1 \right\}. \end{aligned} \quad (19)$$

Lemma 2. System (6) at most two positive equilibria. Moreover,

- (I) if $(a, k_1, k_2) \in \Omega_2$, then system (6) has two positive equilibria: a saddle $E_{11}(x_{11}, y_{11})$, an elementary and antisaddle equilibrium $E_{12}(x_{12}, y_{12})$ ($x_{11} < x_{12}$);

(II)

(i) if $(a, k_1, k_2) \in \Omega_{11}$, then system (6) has a unique positive equilibrium $E_*(x_*, y_*)$, which is degenerate;

(ii) if $(a, k_1, k_2) \in \Omega_{10}$, then system (6) has a unique positive equilibrium $E_{12}(x_{12}, y_{12})$, which is an elementary and antisaddle equilibrium;

(III) if $(a, k_1, k_2) \in \Omega_0$, then system (6) has no positive equilibrium.

Proof. From (17), (18) and the derivative property of $F(x)$, it is easy to see that $\text{Det}(J(E_{11})) < 0$, $\text{Det}(J(E_{12})) > 0$ and $\text{Det}(J(E_*)) = 0$, which implies that E_{11} and E_{12} are all elementary equilibria and E_{11} is a hyperbolic saddle, while E_* is a degenerate equilibrium. ■

Remark 1. From Lemmas 1–2 and Theorem 1, we can know that if $(a, k_1, k_2) \in \Omega_0$ in (19), then system (6) has no positive equilibrium, and $E_{20}(0, k_2)$ is a stable hyperbolic node, or a saddle-node with a stable parabolic sector in the right half plane, or a stable degenerate node of codimension 2. Thus, $E_{20}(0, k_2)$ of system (6) is globally asymptotically stable in the interior of the first quadrant if and only if $(a, k_1, k_2) \in \Omega_0$. Coming back to the original parameters in system (4), we can see that there exists a threshold K_2^* for K_2 (an extra constant carrying capacity coming from other food sources for predators)

$$K_2^* = \begin{cases} \frac{rn}{m}, & 0 < r \leq r^* \triangleq \frac{mhK}{K-n}, \\ \frac{(rK - mhK - rn)^2 + 4nr^2K}{4mrK}, & r > r^*, \end{cases} \tag{20}$$

such that if $K_2 > K_2^*$, then the prey will tend to extinction for all positive initial populations.

Next, we first consider the case (II)(i) in Lemma 2, that is, $(k_1, k_2) \in \widehat{AB}$, and look for some parameters values such that $\text{Tr}(J(E_*)) = 0$. From $F(x_*) = f(x_*) = 0$, we can express x_*, y_* , and k_2 by k_1 and a as follows:

$$k_2 = k_2^* \triangleq \frac{(1 - a - k_1)^2 + 4k_1}{4a}, \quad x_* = \frac{1 - a - k_1}{2}, \quad y_* = \frac{(1 + k_1)^2 - a^2}{4a}, \tag{21}$$

furthermore, from (21) and letting $\text{Tr}(J(E_*)) = 0$, we have

$$k_1 = k_1^* \triangleq \frac{(1 - a)(a - c)}{a + c}. \tag{22}$$

Define

$$a^* = h(c) - c, \quad h(c) = \sqrt{2c(1 + c)}, \tag{23}$$

we have the following results.

Theorem 2. If $(k_1, k_2) \in \widehat{AB}$, that is, $k_2 = k_2^*, k_1 < 1 - a, a < 1$, then system (6) has a unique positive equilibrium $E_*(\frac{1-a-k_1}{2}, \frac{(1+k_1)^2-a^2}{4a})$. Moreover,

- (I) if $k_1 > k_1^*$ (or $0 < k_1 < k_1^*$), then E_* is a saddle-node of codimension 1, which includes a stable (or unstable) parabolic sector;
- (II) if $k_1 = k_1^*$, $a > c$ and
- (i) $a \neq a^*$, then E_* is a cusp of codimension 2;
 - (ii) $a = a^*$, then E_* is a cusp of codimension 3.

Proof. Case (I): $k_2 = k_2^*$ and $k_1 \neq k_1^*$. First, we translate E_* to the origin by $x = u + \frac{1-a-k_1}{2}$, $y = v + \frac{(1+k_1)^2-a^2}{4a}$, then system (6) near the origin takes the form

$$\begin{aligned} \dot{u} &= \frac{a(1-a-k_1)}{1-a+k_1}u - \frac{a(1-a-k_1)}{1-a+k_1}v + \frac{k_1^2+a(2+4k_1)-a^2-1}{(1-a+k_1)^2}u^2 - \frac{4ak_1}{(1-a+k_1)^2}uv \\ &\quad - \frac{4k_1(1+a+k_1)}{(1-a+k_1)^3}u^3 + \frac{8ak_1}{(1-a+k_1)^3}u^2v + o(|u, v|^3), \\ \dot{v} &= cu - cv + \frac{4ac}{a^2-(1+k_1)^2}u^2 - \frac{8ac}{a^2-(1+k_1)^2}uv + \frac{4ac}{a^2-(1+k_1)^2}v^2 + \frac{16a^2c}{(a^2-(1+k_1)^2)^2}u^3 \\ &\quad - \frac{32a^2c}{(a^2-(1+k_1)^2)^2}u^2v + \frac{16a^2c}{(a^2-(1+k_1)^2)^2}uv^2 + o(|u, v|^3). \end{aligned} \quad (24)$$

Next, to make the linear part of system (24) to Jordan form, we make

$$u = X + \frac{a(1-a-k_1)}{c(1-a+k_1)}Y, \quad v = X + Y, \quad t = \frac{(1-a)(a-c) - (a+c)k_1}{1-a+k_1}\tau, \quad (25)$$

then system (24) becomes as (still denote τ by t)

$$\begin{aligned} \dot{X} &= \tilde{a}_{20}X^2 + \tilde{a}_{11}XY + \tilde{a}_{02}Y^2 + \tilde{a}_{30}X^3 + \tilde{a}_{21}X^2Y + \tilde{a}_{12}XY^2 + \tilde{a}_{03}Y^3 + o(|X, Y|^3), \\ \dot{Y} &= Y + \tilde{b}_{20}X^2 + \tilde{b}_{11}XY + \tilde{b}_{02}Y^2 + \tilde{b}_{30}X^3 + \tilde{b}_{21}X^2Y + \tilde{b}_{12}XY^2 + \tilde{b}_{03}Y^3 + o(|X, Y|^3), \end{aligned} \quad (26)$$

where \tilde{a}_{ij} and \tilde{b}_{ij} can be expressed by a, c , and k_1 , and

$$\tilde{a}_{20} = \frac{c(1-a-k_1)(1-a+k_1)}{((1-a)(a-c) - (a+c)k_1)^2} \neq 0 \quad (27)$$

since $k_1 < 1-a$ and $k_1 \neq k_1^*$. Then Theorem 7.1 in chapter 2 of Zhang et al³⁸ implies that E_* is a saddle-node which includes a stable (or unstable) parabolic sector if $k_1 > k_1^*$ (or $0 < k_1 < k_1^*$).

Case (II)(i): when $k_2 = k_2^*$ and $k_1 = k_1^*$, then system (24) can be rewritten as

$$\begin{aligned} \dot{u} &= cu - cv - \frac{c^2 + (1-a)c - a^2}{a(1-a)}u^2 - \frac{a^2 - c^2}{a(1-a)}uv + O(|u, v|^3), \\ \dot{v} &= cu - cv - \frac{c(a+c)^2}{a(1-a)(1+c)}u^2 + \frac{2c(a+c)^2}{a(1-a)(1+c)}uv - \frac{c(a+c)^2}{a(1-a)(1+c)}v^2 + O(|u, v|^3). \end{aligned} \quad (28)$$

Let $u = X + \frac{Y}{c}$, $v = X$, then the linear part of system (28) can be converted to Jordan canonical as following:

$$\begin{aligned} \dot{X} &= Y - \frac{(a+c)^2}{ac(1-a)(1+c)}Y^2 + O(|X, Y|^3), \\ \dot{Y} &= -\frac{c^2}{a}X^2 - \frac{c^2 + 2(1-a)c - a^2}{a(1-a)}XY - \frac{c(1+2c) - ac(1+3c) - (1+2c)a^2}{ac(1-a)(1+c)}Y^2 + O(|X, Y|^3), \end{aligned} \tag{29}$$

by Lemma 3.1 in Ref. 39, system (30) near the origin is equivalent to

$$\begin{aligned} \dot{X} &= Y + O(|X, Y|^3), \\ \dot{Y} &= DX^2 + \check{E}XY + O(|X, Y|^3), \end{aligned} \tag{30}$$

where

$$D = -\frac{c^2}{a}, \quad \check{E} = \frac{a^2 + 2(a-1)c - c^2}{a(1-a)}. \tag{31}$$

Obviously, $D \neq 0$. If $a \neq a^*$, then $\check{E} \neq 0$, hence E_* is a cusp of codimension 2; If $a = a^*$, then E_* is a cusp of codimension at least 3. Next we confirm that E_* is a cusp of codimension exactly 3.

Case (II)(ii): when $k_2 = k_2^*, k_1 = k_1^*$ and $a = a^*$, then system (24) can be written as

$$\begin{aligned} \dot{u} &= \check{a}_{10}u + \check{a}_{01}v + \check{a}_{20}u^2 + \check{a}_{11}uv + \check{a}_{30}u^3 + \check{a}_{21}u^2v + \check{a}_{40}u^4 + \check{a}_{31}u^3v + o(|u, v|^4), \\ \dot{v} &= \check{b}_{10}u + \check{b}_{01}v + \check{b}_{20}u^2 + \check{b}_{11}uv + \check{b}_{02}v^2 + \check{b}_{30}u^3 + \check{b}_{21}u^2v + \check{b}_{12}uv^2 + \check{b}_{40}u^4 \\ &\quad + \check{b}_{31}u^3v + \check{b}_{22}u^2v^2 + o(|u, v|^4), \end{aligned} \tag{32}$$

where \check{a}_{ij} and \check{b}_{ij} are given in Appendix A.

Letting $X = u$, $Y = w$, where w denotes the right side of the first equation of (32), then we have

$$\begin{aligned} \dot{X} &= Y, \\ \dot{Y} &= \check{c}_1X^2 + \check{c}_2Y^2 + \check{c}_3X^3 + \check{c}_4X^2Y + \check{c}_5XY^2 + \check{c}_6X^4 + \check{c}_7X^3Y + \check{c}_8X^2Y^2 + o(|X, Y|^4), \end{aligned} \tag{33}$$

where \check{c}_i are given in Appendix A.

To eliminate Y^2 -term in (33), let

$$x = X, \quad y = (1 - \check{c}_2X)Y, \quad t = (1 - \check{c}_2X)\tau, \tag{34}$$

then system (33) becomes(still denote τ by t)

$$\begin{aligned} \dot{x} &= y, \\ \dot{y} &= \check{d}_1x^2 + \check{d}_2x^3 + \check{d}_3x^2y + \check{d}_4xy^2 + \check{d}_5x^4 + \check{d}_6x^3y + \check{d}_7x^2y^2 + o(|x, y|^4), \end{aligned} \tag{35}$$

where

$$\check{d}_1 = \check{c}_1, \quad \check{d}_2 = \check{c}_3 - 2\check{c}_1\check{c}_2, \quad \check{d}_3 = \check{c}_4, \quad \check{d}_4 = \check{c}_5 - \check{c}_2^2, \quad (36)$$

$$\check{d}_5 = \check{c}_1\check{c}_2^2 + \check{c}_6 - 2\check{c}_2\check{c}_3, \quad \check{d}_6 = \check{c}_7 - \check{c}_2\check{c}_4, \quad \check{d}_7 = \check{c}_8 - \check{c}_2^3. \quad (37)$$

Note that $\check{d}_1 = \check{c}_1 = -\frac{c^2}{\sqrt{2c(1+c)}-c} < 0$, let

$$X = -x, \quad Y = -\frac{y}{\sqrt{-\check{d}_1}}, \quad \tau = \sqrt{-\check{d}_1}t, \quad (38)$$

then system (35) becomes (still denote τ by t)

$$\begin{aligned} \dot{X} &= Y, \\ \dot{Y} &= X^2 - \frac{\check{d}_2}{\check{d}_1}X^3 + \frac{\check{d}_3}{\sqrt{-\check{d}_1}}X^2Y + \check{d}_4XY^2 + \frac{\check{d}_5}{\check{d}_1}X^4 - \frac{\check{d}_6}{\sqrt{-\check{d}_1}}X^3Y - \check{d}_7X^2Y^2 + o(|X, Y|^4). \end{aligned} \quad (39)$$

By the Proposition 5.3 in Lamontagne et al,⁴⁰ the equivalent system of system (39) near the origin takes the following form:

$$\begin{aligned} \dot{X} &= Y, \\ \dot{Y} &= X^2 + MX^3Y + o(|X, Y|^4), \end{aligned} \quad (40)$$

where

$$M = -\frac{(a^* - c)(2 + c - a^*)(a^* + c)^2}{c(1 + c)(1 - a^*)^2\sqrt{a^{*5}}}. \quad (41)$$

Obviously, we have $M < 0$ for $0 < c < a^* < 1$. Hence E_* is a cusp of codimension exactly 3 when $k_2 = k_2^*, k_1 = k_1^*$, and $a = a^*$. ■

2.2 | Hopf bifurcation with codimension up to 2

From Lemma 2, we know that E_{12} is a center-type equilibrium when $\text{Tr}(J(E_{12})) = 0$ and system (6) may undergo Hopf bifurcation around E_{12} . In this subsection, we show that the center-type equilibrium E_{12} is a weak focus with order up to 2 when $\text{Tr}(J(E_{12})) = 0$, and the highest codimension of Hopf bifurcation around E_{12} is 2.

To simplify the subsequent calculation, we denote x_{12} by z , then $E_{12}(x_{12}, y_{12})$ becomes as $E_{12}(z, k_2 + z)$. From $F(z) = 0$ and $\text{Tr}(J(E_{12})) = 0$, k_1 and k_2 can be expressed by a, c , and z as

follows:

$$k_1 = k_1^H \triangleq \frac{(1 - c - 2z)}{c + z}, \quad k_2 = k_2^H \triangleq z \frac{(1 - z)^2 - a(c + z)}{a(c + z)}. \quad (42)$$

Define

$$\mathcal{T} := \left\{ (a, c, z) \in \mathbb{R}_+^3 : \frac{c(1 - z)}{c + z} < a < \frac{(1 - z)^2}{c + z}, 0 < z < \frac{1 - c}{2}, 0 < c < 1 \right\}, \quad (43)$$

which comes from $k_1^H > 0$, $k_2^H > 0$ in (42) and $\text{Det}(J(E_{12})) > 0$.

Next, when $(a, c, z) \in \mathcal{T}$ and (42) hold, we calculate the focal values around $E_{12}(z, k_2 + z)$ of system (6). We first make the following transformations successively:

$$\begin{aligned} t &= (k_1 + x)(k_2 + x)\tau; \\ x &= u + z, \quad y = v + k_2 + z; \end{aligned} \quad (44)$$

$$u = -\frac{\hat{A}_{10}\hat{A}_{01}}{\hat{A}_{10}^2+d}X - \frac{\hat{A}_{01}\sqrt{d}}{\hat{A}_{10}^2+d}Y, \quad v = X, \quad \tau = \sqrt{dt},$$

where

$$\hat{A}_{10} = \frac{c(1 - z)^3 z^2}{a(c + z)^2}, \quad \hat{A}_{01} = -\frac{(1 - z)^2 z^2}{c + z}, \quad d = \hat{A}_{10}\hat{B}_{01} - \hat{B}_{10}\hat{A}_{01}, \quad (45)$$

$$\hat{B}_{10} = \frac{c(1 - z)^3 z^2}{a(c + z)^2}, \quad \hat{B}_{01} = -\frac{c(1 - z)^3 z^2}{a(c + z)^2}, \quad (46)$$

then system (6) becomes

$$\begin{aligned} \dot{X} &= Y + \hat{C}_{11}XY + \hat{C}_{02}Y^2 + \hat{C}_{21}X^2Y + \hat{C}_{12}XY^2, \\ \dot{Y} &= -X + \hat{D}_{20}X^2 + \hat{D}_{11}XY + \hat{D}_{02}Y^2 + \hat{D}_{30}X^3 + \hat{D}_{21}X^2Y + \hat{D}_{12}XY^2 + \hat{D}_{03}Y^3 \\ &\quad + \hat{D}_{40}X^4 + \hat{D}_{31}X^3Y + \hat{D}_{22}X^2Y^2 + \hat{D}_{13}XY^3 + \hat{D}_{04}Y^4, \end{aligned} \quad (47)$$

where k_1, k_2 have been eliminated by (42), and the coefficients are given in Appendix B.

According to formal series method in Ref. 38, we can get the first two focal values (or Lyapunov coefficients) as follows:

$$\begin{aligned} \sigma_1 &= -\frac{a(c + z)^2 f_1}{z^2(1 - z)^2(c(1 - z)(az - c + ac + zc))^{\frac{3}{2}}}, \\ \sigma_2 &= \frac{a(c + z)^2 f_2}{z^4(1 - z)^5(c(1 - z)(az - c + ac + zc))^{\frac{7}{2}}}, \end{aligned} \quad (48)$$

where

$$\begin{aligned}
 f_1 = & a^2c^3 + 5a^2c^2z - a^2c^2 + 6a^2cz^2 - a^2cz + 2a^2z^3 + 2ac^3z - 2ac^3 + 9ac^2z^2 - 11ac^2z \\
 & + 2ac^2 + 10acz^3 - 13acz^2 + 3acz + 4az^4 - 6az^3 + 2az^2 + c^3z^2 - 2c^3z + c^3 + 3c^2z^3 \quad (49) \\
 & - 7c^2z^2 + 5c^2z - c^2 - cz^3 + 2cz^2 - cz - 2z^5 + 4z^4 - 2z^3,
 \end{aligned}$$

and f_2 is given in Appendix B.

Let $\text{lcoeff}(\xi, x)$ be the leading coefficient of ξ with respect to x , then

$$\text{lcoeff}(f_1, a) = (c + z)r_1, \quad (50)$$

where

$$r_1 = 2z^2 + 4cz + c(c - 1). \quad (51)$$

It is easy to see that $r_1 = 0$ if and only if $z = z^*$, where

$$z^* = \frac{\sqrt{2c(1+c)} - 2c}{2}. \quad (52)$$

When $z = z^*$, we have the following results.

Lemma 3. *If $(a, c, z) \in \mathcal{T}$, $z = z^*$ and (42) hold, then E_{12} is a stable weak focus of order 1.*

Proof. Substituting $z = z^*$ into f_1 , we have

$$f_1 = \frac{c(1+c)((2+7c)\sqrt{1+c} - (4+5c)\sqrt{2c})f_{11}}{2\sqrt{2c}}, \quad (53)$$

where

$$f_{11} = a\sqrt{2c(1+c)} - c(2+2c - \sqrt{2c(1+c)}). \quad (54)$$

Since $z = z^*$ and $(a, c, z) \in \mathcal{T}$, we have $\frac{c(2+2c-\sqrt{2c(1+c)})}{\sqrt{2c(1+c)}} < a < \frac{(2+2c-\sqrt{2c(1+c)})^2}{2\sqrt{2c(1+c)}}$, which implies $f_{11} > 0$. Moreover, $(2+7c)\sqrt{1+c} - (4+5c)\sqrt{2c} > 0$ for $0 < c < 1$. Thus, $f_1 > 0$, that is, $\sigma_1 < 0$, then E_{12} is a stable weak focus of order 1. \blacksquare

Let

$$V(f_1, f_2) := \{(a, c, z) \in \mathbb{R}^3 : f_1 = 0, f_2 = 0\}. \quad (55)$$

When $z \neq z^*$, we have the main results of this subsection.

Lemma 4. *If $z \neq z^*$, then $V(f_1, f_2) \cap \mathcal{T} = \emptyset$.*

Proof. If $z \neq z^*$, then $\text{lcoeff}(f_1, a) \neq 0$ for $(a, c, z) \in \mathcal{T}$. Using MAPLE command “resultant,” we compute the resultant of f_1 and f_2 with respect to a ³⁶

$$r_{12} := \text{res}(f_1, f_2, a) = 16c^2z^4(z - 1)^{14}(c + z)^{13}(c + 2z - 1)^3(c + 2z)^3r_1^3r_2r_3, \tag{56}$$

where r_1 is given in (51), and

$$\begin{aligned} r_2 &= c^2 + 2cz - c - 2z^2, \\ r_3 &= c^6 + 6c^5z - 6c^5 - 9c^4z^2 - 36c^4z + 13c^4 - 144c^3z^3 - 12c^3z^2 + 48c^3z \\ &\quad - 12c^3 - 342c^2z^4 + 162c^2z^3 + 9c^2z^2 - 18c^2z + 4c^2 - 288cz^5 + 198cz^4 - 54cz^3 \\ &\quad + 12cz^2 - 72z^6 + 36z^5. \end{aligned} \tag{57}$$

When $z \neq z^*$ and $(a, c, z) \in \mathcal{T}$, it is easy to check that all the factors, except r_3 , in r_{12} are not equal to zero. Next, we will prove $r_3 > 0$ for $(a, c, z) \in \mathcal{T}$.

We treat r_3 as the function of z , that is, $r_3 =: r_3(z)$. Since $(a, c, z) \in \mathcal{T}$, then $0 < z < \frac{1-c}{2}$ and $0 < c < 1$. Notice that $r_3(0) = c^2(1 - c)^2(2 - c)^2 > 0$ and $r_3(\frac{1-c}{2}) = \frac{1}{4}c(3 + c)(1 - c^2)^2 > 0$ for $0 < c < 1$, then Lemma 3.1 in Yang³⁷ indicates that the number of zeros for $r_3(z)$ in the interval $(0, \frac{1-c}{2})$ is equal to that of positive zeros for

$$\Phi(z) := (1 + z)^6r_3\left(\frac{1 - c}{2(1 + z)}\right) = \frac{(1 - c)^2Q(z)}{8} \tag{58}$$

in $(0, \frac{1-c}{2})$, where

$$\begin{aligned} Q(z) &= 8c^2(2 - c)^2z^6 + 24c^2(c^2 - 3c + 5)z^5 + 6c(c + 1)(4 + 19c - 3c^2)z^4 + 2c(21 - c)(1 + c) \\ &\quad (1 + 4c)z^3 + 3c(c + 1)(11c^2 + 22c + 27)z^2 + 3(c + 1)^2(6c^2 + 5c + 3)z + 2c(3 + c)(c + 1)^2. \end{aligned} \tag{59}$$

It is easy to see that $Q(z) > 0$ for any $z > 0$ since $0 < c < 1$, then $\Phi(z) > 0$ holds for $z > 0$, which means $\Phi(z)$ has no positive zeros, that is, $r_3(z)$ has no zeros in $(0, \frac{1-c}{2})$. Then $r_3 = r_3(z) > 0$ for $(a, c, z) \in \mathcal{T}$. Thus, $V(r_{12}) \cap \mathcal{T} = \emptyset$. By the results in p. 398 in Ref. 36 we have $V(f_1, f_2) \cap \mathcal{T} = \emptyset$. ■

Denote

$$\mathcal{T}_1 := \{(a, c, z) \in \mathcal{T} \mid \sigma_1 \neq 0\}, \quad \mathcal{T}_2 := \{(a, c, z) \in \mathcal{T} \mid \sigma_1 = 0\}. \tag{60}$$

Theorem 3. *Let (42) hold, and*

- (i) *if $(a, c, z) \in \mathcal{T}_1$, then E_{12} is a weak focus of order 1;*
- (ii) *if $(a, c, z) \in \mathcal{T}_2$, then E_{12} is a weak focus of order 2.*

Proof. According to Lemmas 5 and 4, E_{12} is a weak focus of order at most 2 if $(a, c, z) \in \mathcal{T}$ and (42) hold. If $(a, c, z) \in \mathcal{T}_1$, then $\sigma_1 \neq 0$, which means E_{12} is a weak focus of order 1. If $(a, c, z) \in \mathcal{T}_2$, then we have $\sigma_1 = 0$ and $\sigma_2 \neq 0$, which means E_{12} is a weak focus of order 2. ■

We next provide three sets of parameters such that E_{12} is a stable (or an unstable) weak focus of order 1, or a stable weak focus of order 2, respectively, correspondingly, system (6) can undergo supercritical (or subcritical) Hopf bifurcation or Hopf bifurcation of codimension 2.

In Figure 2A, when $(a, c, k_1, k_2) = (\frac{1}{2}, \frac{1}{4}, \frac{1}{8} + 0.001, \frac{5}{16})$, there exists an unstable limit cycle bifurcating from subcritical Hopf bifurcation and system (6) undergoes bistability phenomenon (two stable equilibria E_{20}, E_{12}). In Figure 2B, when $(a, c, k_1, k_2) = (1, \frac{1}{4}, \frac{1}{8} - 0.02, \frac{1}{32})$, there exists a stable limit cycle bifurcating from supercritical Hopf bifurcation.

Finally, we provide two examples to show the existence of two limit cycles around E_{12} . (i) Two limit cycles bifurcating from Hopf bifurcation of codimension 2 (see Figure 2C–D). It is easy to check that $E_{12}(\frac{1}{10}, \frac{9(1+\sqrt{257})}{1280})$ is a stable weak focus of order 2 when $(a, c, k_1, k_2) = (\frac{9(\sqrt{257}-1)}{160}, \frac{7}{10}, \frac{1}{80}, \frac{9\sqrt{257}-119}{1280})$, and

$$\left| \frac{\partial(\text{Tr}(J(E_{12})), \sigma_1)}{\partial(a, c)} \right|_{(a, c, k_1, k_2) = (\frac{9(\sqrt{257}-1)}{160}, \frac{7}{10}, \frac{1}{80}, \frac{9\sqrt{257}-119}{1280})} = -\frac{320\sqrt{2}(41\sqrt{257}-359)}{63(\sqrt{257}-1)\sqrt{7(\sqrt{257}-15)^5}} \quad (61)$$

$$\doteq -49.8916,$$

which means that system (6) can undergo Hopf bifurcation of codimension 2. In Figure 2C–D, system (6) can undergo two limit cycles and tristability phenomenon (two stable equilibria E_{20}, E_{12} and a stable limit cycle). (ii) Two limit cycles: the inner one bifurcating from subcritical Hopf bifurcation, the outer one coming from Poincaré–Bendixson Theorem (Figure 2E–F). Letting $(a, c, k_1, k_2) = (2, \frac{1}{5}, \frac{7}{50}, \frac{161}{400})$, then we have $\text{Tr}(J(E_{12})) = 0$, $\text{Det}(J(E_{12})) = \frac{31}{475} > 0$, $\sigma_1 = \frac{85312500}{212629\sqrt{589}} > 0$, which implies that E_{12} is an unstable weak focus of order 1. Next, we decrease k_1 to $\frac{7}{50} - 0.0001$, then at least two limit cycles occur: an unstable limit cycle (inner) by subcritical Hopf bifurcation and at least a stable limit cycle (outer) by Poincaré–Bendixson Theorem (see Figure 2E–F), which means that the unique positive equilibrium E^* is not globally asymptotically stable when it is locally asymptotically stable, and system (6) undergoes bistability phenomenon (one stable equilibrium E_{12} and one stable limit cycle).

From Theorem 6 and the above results, we have the main theorem in this subsection.

Theorem 4. *The highest codimension of Hopf bifurcation around E_{12} in system (6) is 2. Two limit cycles can bifurcate from Hopf bifurcation of codimension 2, the inner one is unstable.*

2.3 | Degenerate Bogdanov–Takens bifurcation of codimension 3

From Theorem 2, we know that system (6) may exhibit a degenerate Bogdanov–Takens bifurcation of codimension 3 around E_* if the bifurcation parameters are chosen appropriately. To make sure if such a bifurcation can be fully unfolded inside the class of system (6), we choose a , k_1 , and k_2

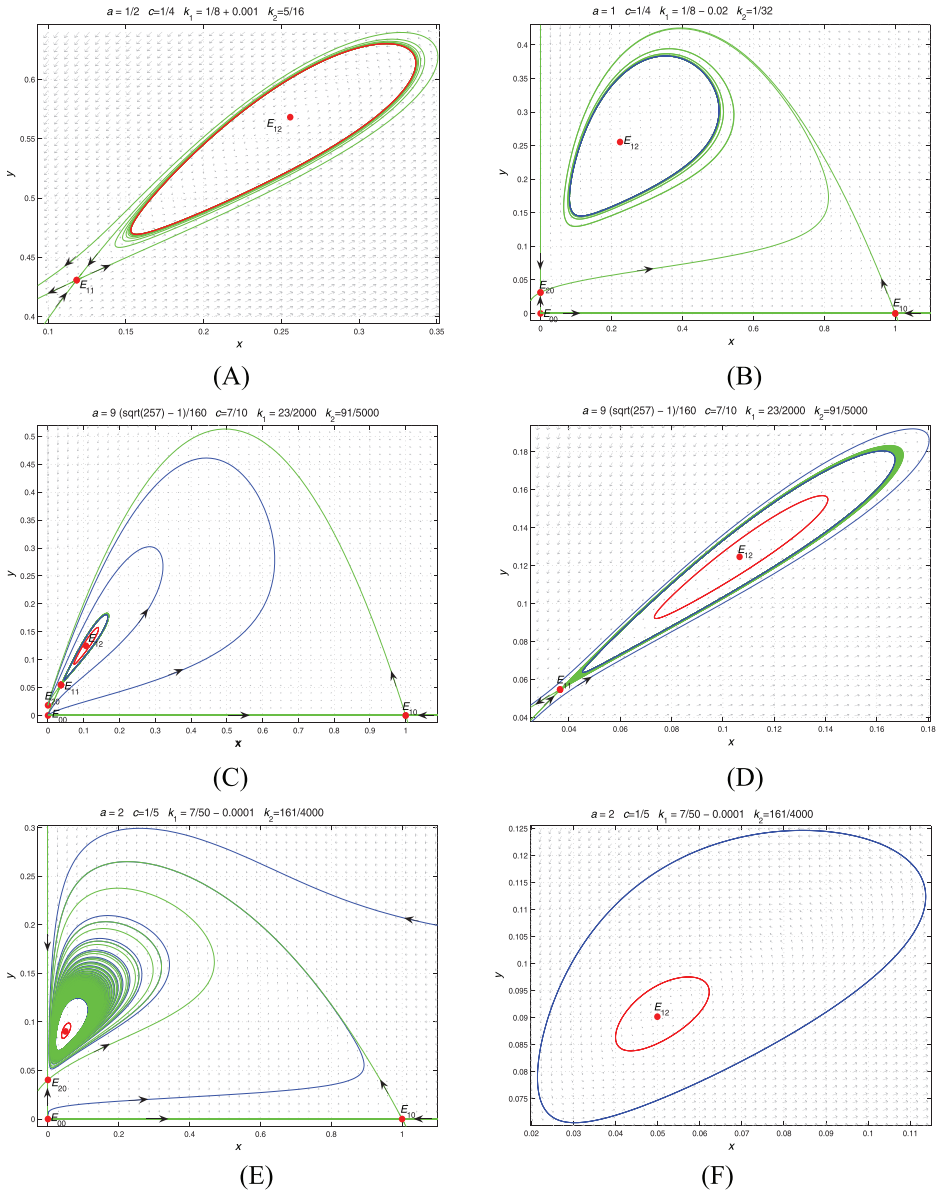


FIGURE 2 (A) An unstable limit cycle by subcritical Hopf bifurcation. (B) A stable limit cycle by supercritical Hopf bifurcation. (C)–(D) Two limit cycles by degenerate Hopf bifurcation, the inner one is unstable. (E)–(F) Two limit cycles, the inner one from subcritical Hopf bifurcation, the outer one from Poincaré–Bendixon Theorem

as bifurcation parameters and obtain the following unfolding system:

$$\begin{aligned} \dot{x} &= \left(1 - x - \frac{(a^* + \eta_1)y}{k_1^* + \eta_2 + x} \right), \\ \dot{y} &= cy \left(1 - \frac{y}{k_2^* + \eta_3 + x} \right), \end{aligned} \tag{62}$$

where k_2^*, k_1^*, a^* are given in (21), (22), (23), respectively, and $\eta = (\eta_1, \eta_2, \eta_3) \sim (0, 0, 0)$. We will transform system (62) into the following system by a series of near-identity transformations⁴¹:

$$\begin{aligned}\dot{x} &= y, \\ \dot{y} &= \mu_1 + \mu_2 y + \mu_3 xy + x^2 \pm x^3 y + R(x, y, \mu),\end{aligned}\quad (63)$$

where

$$R(x, y, \mu) = y^2 O(|x, y|^2) + O(|x, y|^5) + O(\mu)(O(|y|^2) + O(|x, y|^3)) + O(\mu^2)O(|x, y|), \quad (64)$$

and check $\left. \frac{\partial(\mu_1, \mu_2, \mu_3)}{\partial(\eta_1, \eta_2, \eta_3)} \right|_{\eta=0} \neq 0$.

Theorem 5. *System (6) undergoes a degenerate Bogdanov–Takens bifurcation of codimension 3 around E_* as (a, k_1, k_2) varying in the small neighborhood of (a^*, k_1^*, k_2^*) , where the cusp of codimension 3 acts as the “organizing center” for the bifurcation diagram. More precisely, there exist a series of bifurcation with lower codimension which are subordinate to a cusp of codimension 3, such as:*

- (i) *Codimension-1: Hopf bifurcation, homoclinic bifurcation, saddle-node bifurcation of limit cycle, and saddle-node bifurcation;*
- (ii) *Codimension-2: degenerate Hopf bifurcation, Bogdanov–Takens bifurcation, degenerate homoclinic bifurcation, and Hopf and homoclinic bifurcation simultaneously.*

Proof. Firstl, let $X = x - \frac{c(1-a^*)}{a^*+c}$, $Y = y - \frac{a^*(1-a^*)(1+c)}{(a^*+c)^2}$, then the Taylor expansion of the system (62) near the origin takes the form

$$\begin{aligned}\dot{X} &= A_{00} + A_{10}X + A_{01}Y + A_{20}X^2 + A_{11}XY + A_{30}X^3 + A_{21}X^2Y + A_{40}X^4 + A_{31}X^3Y \\ &\quad + o(|X, Y|^4), \\ \dot{Y} &= B_{00} + B_{10}X + B_{01}Y + B_{20}X^2 + B_{11}XY + B_{02}Y^2 + B_{30}X^3 + B_{21}X^2Y + B_{12}XY^2 \\ &\quad + B_{40}X^4 + B_{31}X^3Y + B_{22}X^2Y^2 + o(|X, Y|^4),\end{aligned}\quad (65)$$

where the coefficients are given in Appendix B.

Second, let $x = X$, $y = \dot{X}$, then system (65) can be rewritten as

$$\begin{aligned}\dot{x} &= y, \\ \dot{y} &= C_{00} + C_{10}x + C_{01}y + C_{20}x^2 + C_{11}xy + C_{02}y^2 + C_{30}x^3 + C_{21}x^2y + C_{12}xy^2 + C_{40}x^4 \\ &\quad + C_{31}x^3y + C_{22}x^2y^2 + o(|x, y|^4),\end{aligned}\quad (66)$$

where C_{ij} can be expressed by A_{ij} and B_{ij} , we omit them for brevity, the same for the following.

Next, following the produce in Ref. 42 (see also Ref. 43), we use seven steps to transform system (66) into system (63).

(I) **Eliminating the y^2 -term in system (66).** Let $x = X + \frac{C_{02}}{2}X^2$, $y = Y + C_{02}XY$, then system (66) can be rewritten as

$$\begin{aligned} \dot{X} &= Y, \\ \dot{Y} &= D_{00} + D_{10}X + D_{01}Y + D_{20}X^2 + D_{11}XY + D_{30}X^3 + D_{21}X^2Y + D_{12}XY^2 \\ &\quad + D_{40}X^4 + D_{31}X^3Y + D_{22}X^2Y^2 + o(|X, Y|^4). \end{aligned} \tag{67}$$

(II) **Eliminating the XY^2 -term in system (67).** Let $X = x + \frac{D_{12}}{6}x^3$, $Y = y + \frac{D_{12}}{2}x^2y$, then system (67) is changed into

$$\begin{aligned} \dot{x} &= y, \\ \dot{y} &= \tilde{E}_{00} + \tilde{E}_{10}x + \tilde{E}_{01}y + \tilde{E}_{20}x^2 + \tilde{E}_{11}xy + \tilde{E}_{30}x^3 + \tilde{E}_{21}x^2y + \tilde{E}_{40}x^4 \\ &\quad + \tilde{E}_{31}x^3y + \tilde{E}_{22}x^2y^2 + o(|x, y|^4). \end{aligned} \tag{68}$$

(III) **Eliminating the x^3 -term and x^4 -term in system (68).** It is not hard to find that $\tilde{E}_{20} = -\frac{c^2}{a^*} + O(\eta) < 0$ for small η . Let

$$x = X - \frac{\tilde{E}_{30}}{4\tilde{E}_{20}}X^2 + \frac{15\tilde{E}_{30}^2 - 16\tilde{E}_{20}\tilde{E}_{40}}{80\tilde{E}_{20}^2}X^3, \quad y = Y, \quad t = \left(1 - \frac{\tilde{E}_{30}}{2\tilde{E}_{20}}X + \frac{45\tilde{E}_{30}^2 - 48\tilde{E}_{20}\tilde{E}_{40}}{80\tilde{E}_{20}^2}X^2 \right)\tau, \tag{69}$$

then system (68) becomes (still denote τ by t)

$$\begin{aligned} \dot{X} &= Y, \\ \dot{Y} &= F_{00} + F_{10}X + F_{01}Y + F_{20}X^2 + F_{11}XY + F_{30}X^3 + F_{21}X^2Y + F_{40}X^4 \\ &\quad + F_{31}X^3Y + P_1(X, Y, \eta), \end{aligned} \tag{70}$$

where $P_1(X, Y, \eta)$ has the property of (64), and $F_{40} = F_{30} = 0$ when $\eta = 0$.

(IV) **Eliminating the X^2Y -term in system (70).** Notice that $F_{20} = -\frac{c^2}{a^*} + O(\eta) < 0$ when η sufficient small. Let

$$X = x, \quad Y = y + \frac{F_{21}}{3F_{20}}y^2 + \frac{F_{21}^2}{36F_{20}^2}y^3, \quad t = \left(1 + \frac{F_{21}}{3F_{20}}y + \frac{F_{21}^2}{36F_{20}^2}y^2 \right)\tau, \tag{71}$$

then system (70) can be rewritten as (still denote τ by t)

$$\begin{aligned} \dot{x} &= y, \\ \dot{y} &= G_{00} + G_{10}x + G_{01}y + G_{20}x^2 + G_{11}xy + G_{31}x^3y + P_2(x, y, \eta), \end{aligned} \tag{72}$$

where $P_2(x, y, \eta)$ has the property of (64).

(V) **Reduce the coefficients of x^2 and x^3y to 1 and -1 in system (72), respectively.** Notice that $G_{20} = -\frac{c^2}{a^*} + O(\eta) < 0$, $G_{31} = \frac{4c(1+c)(h(c)-5c(1-h(c))-7c^2)}{(a^*-(a^*)^2)^3} + O(\eta) > 0$ for small η . Let

$$x = G_{20}^{\frac{1}{5}} G_{31}^{-\frac{2}{5}} X, \quad y = -G_{20}^{\frac{4}{5}} G_{31}^{-\frac{3}{5}} Y, \quad t = -G_{20}^{-\frac{3}{5}} G_{31}^{\frac{1}{5}} \tau, \quad (73)$$

then system (72) becomes (still denote τ by t)

$$\begin{aligned} \dot{X} &= Y, \\ \dot{Y} &= H_{00} + H_{10}X + H_{01}Y + X^2 + H_{11}XY - X^3Y + P_3(X, Y, \eta), \end{aligned} \quad (74)$$

where $P_3(X, Y, \eta)$ has the property of (64).

(VI) **Eliminating the X -term in system (74).** Let $x = X + \frac{H_{10}}{2}$, $y = Y$, then system (74) can be rewritten as

$$\begin{aligned} \dot{x} &= y, \\ \dot{y} &= \mu_1 + \mu_2y + x^2 + \mu_3xy - x^3y + P_4(x, y, \eta), \end{aligned} \quad (75)$$

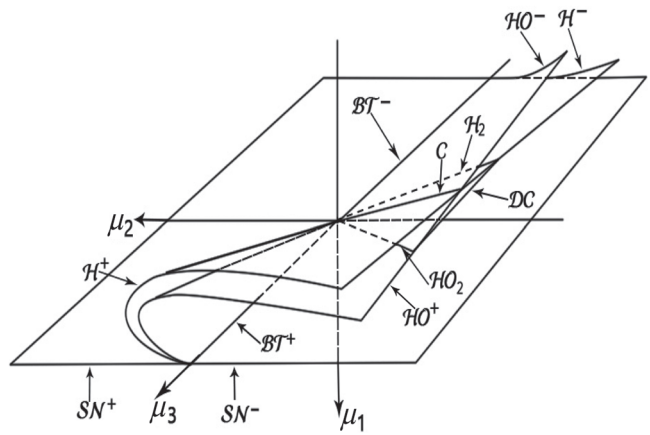
where $P_4(x, y, \eta)$ has the property of (64), and

$$\begin{aligned} \mu_1 &= \frac{(a^* - 1)\sqrt[5]{8a^{*7}H_1^4}}{c}\eta_1 - \frac{2(1+c)\sqrt[5]{8a^{*7}H_1^4}}{h(c)}\eta_2 + 2\sqrt[5]{8a^{*7}H_1^4}\eta_3 + o(\eta), \\ \mu_2 &= -\frac{\sqrt{2(1+c)}H_2\sqrt[5]{4H_1}}{c^2H_5\sqrt[5]{a^{*2}}}\eta_1 + \frac{H_3\sqrt[5]{4H_1}}{cH_6\sqrt[5]{a^{*2}}}\eta_2 + \frac{2H_4\sqrt[5]{4H_1}}{H_6\sqrt[5]{a^{*2}}}\eta_3 + o(\eta), \\ \mu_3 &= -\frac{(1+c)h(c)H_7}{cH_{10}H_5^2\sqrt[5]{4a^{*8}H_1}}\eta_1 - \frac{(1+c)H_8}{H_5^3H_{10}\sqrt[5]{4a^{*8}H_1}}\eta_2 + \frac{H_9\sqrt[5]{8a^{*7}H_1^4}}{H_{10}^2}\eta_3 + o(\eta), \end{aligned} \quad (76)$$

in which

$$\begin{aligned} H_1 &= \frac{(1+c)(h(c)+5ch(c)-5c-7c^2)}{(h(c)+2ch(c)-3c-3c^2)^3}, \quad H_2 = 2h(c)c + h(c) - 3c^2 - 3c, \\ H_3 &= 3h(c)c + 2h(c) - 5c^2 - 5c, \quad H_4 = 3h(c) - 4c - 2, \quad H_5 = h(c) - c - 1, \\ H_6 &= 2h(c) - 3c - 1, \quad H_7 = 70h(c)c^2 + 64h(c)c + 10h(c) - 99c^3 - 140c^2 - 47c - 2, \\ H_8 &= 145h(c)c^3 + 245h(c)c^2 + 121h(c)c + 17h(c) - 205c^4 - 449c^3 - 319c^2 - 79c - 4, \\ H_9 &= 181h(c)c^3 + 198h(c)c^2 + 51h(c)c + 2h(c) - 256c^4 - 408c^3 - 180c^2 - 20c, \\ H_{10} &= 5h(c)c + h(c) - 7c^2 - 5c. \end{aligned} \quad (77)$$

FIGURE 3 Bifurcation diagram for Bogdanov–Takens bifurcation of codimension 3



Finally, by MATHEMATICA software, we have

$$\left| \frac{D(\mu_1, \mu_2, \mu_3)}{D(\eta_1, \eta_2, \eta_3)} \right|_{\eta=0} = \frac{4\sqrt[5]{8c(1+c)^3}H_{11}}{\sqrt[5]{cG_{20}^2(0)H_1a^{*4}(1-a^*)^7}}, \tag{78}$$

where $0 < c < a^* < 1$,

$$H_{11} = 140c^4 + (268 - 99h(c))c^3 + 4(37 - 35h(c))c^2 + (20 - 47h(c))c + 2h(c), \tag{79}$$

and $h(c)$ is given in (23). We can check that $H_{11}(c) \neq 0$ for $c \in (0, 1)$. In fact, let $H_{11}(c) = 0$, after simplification, we can obtain $2c(1+c)(2+c)^2(1-c)^4 = 0$, that is, $c = 1$, which is contradict with $c \in (0, 1)$. Similarly, we also have $H_1 \neq 0$. Thus, the nondegenerate condition $\left| \frac{D(\mu_1, \mu_2, \mu_3)}{D(\eta_1, \eta_2, \eta_3)} \right|_{\eta=0} \neq 0$ holds for small η . According to Dumortier et al⁴¹ system (75) is the versal unfolding of Bogdanov–Takens singularity (cusp case) of codimension 3. The remainder term $P_4(x, y, \eta)$, with the property of (64), does not affect the bifurcation phenomena, and the dynamics of system (6) around E_* as (a, k_1, k_2) changes near (a^*, k_1^*, k_2^*) are equivalent to that of system (75) around $(0,0)$ as (μ_1, μ_2, μ_3) varies near $(0,0,0)$. ■

According to Figure 6 in Lamontagne et al,⁴⁰ we plot the bifurcation diagram for system (75) in Figure 3, the description for the notations are given in Table 1.

Note that system (75) has no equilibria for $\mu_1 > 0$. Hence, all the bifurcation surfaces (curves) are in the half-space $\mu_1 < 0$. Figure 3 can be best visualized by drawing their intersections with the half sphere

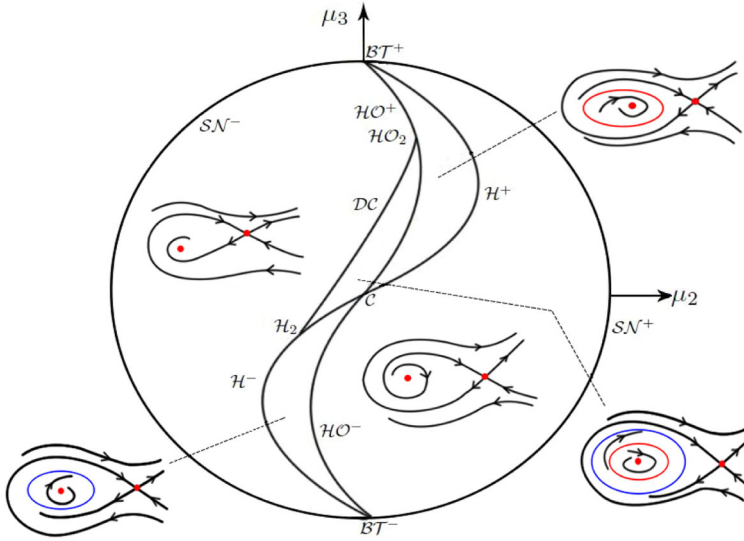
$$S = \{(\mu_1, \mu_2, \mu_3) | \mu_1^2 + \mu_2^2 + \mu_3^2 = \varepsilon^2, \mu_1 \leq 0, \varepsilon > 0 \text{ sufficiently small}\}. \tag{80}$$

To see the intersections more clearly, we project the intersections onto (μ_2, μ_3) -plane and plot phase portraits in each regions in Figure 4.

Now we summarize the bifurcation phenomena of system (75), which is equivalent to the original system (6). There are four bifurcation curves: SN (saddle-node bifurcation curve), HO (homoclinic bifurcation curve), H (Hopf bifurcation curve), and DC (saddle-node bifurcation

TABLE 1 Caption of notations in Figure 3

Caption	Notation
\mathcal{H}^+	Subcritical Hopf bifurcation
\mathcal{H}^-	Supercritical Hopf bifurcation
\mathcal{HO}^+	Repelling Homoclinic bifurcation
\mathcal{HO}^-	Attracting Homoclinic bifurcation
\mathcal{H}_2	Hopf bifurcation of codimension 2
\mathcal{HO}_2	Homoclinic bifurcation of codimension 2
C	Intersect of \mathcal{H} and \mathcal{HO}
DC	Saddle-node bifurcation of limit cycle
BT^+	Subcritical Bogdanov–Takens bifurcation
BT^-	Supercritical Bogdanov–Takens bifurcation
$S\mathcal{N}^+$	Saddle-node with an unstable parabolic sector
$S\mathcal{N}^-$	Saddle-node with a stable parabolic sector

FIGURE 4 The projection of the intersections of Figure 3 with the half sphere S

curve of limit cycles). The curve DC is tangent to \mathcal{H} at a point \mathcal{H}_2 and tangent to \mathcal{HO} at a point \mathcal{HO}_2 . The curves \mathcal{H} and C have first-order contact with $S\mathcal{N}$ at the points BT^+ and BT^- . In the neighborhood of BT^+ and BT^- , system (75) undergoes Bogdanov–Takens bifurcations of codimension 2. And the detail bifurcations are listed as follows:

- (1) Codimension-1 bifurcations: Hopf bifurcation \mathcal{H} (except at the point \mathcal{H}_2), homoclinic bifurcation \mathcal{HO} (except the point \mathcal{HO}_2), saddle-node bifurcation of limit cycle DC (except the points \mathcal{HO}_2 and \mathcal{H}_2);
- (2) Codimension-2 bifurcations: degenerate Hopf bifurcation \mathcal{H}_2 , Bogdanov–Takens bifurcation BT^+ and BT^- , degenerate homoclinic bifurcation \mathcal{HO}_2 , Hopf and homoclinic bifurcation simultaneously C .

FIGURE 5 Bifurcation diagram of system (6) in (k_1, a) plane when $(c, k_2) = (\frac{2}{5}, \frac{6}{50})$. The blue and red solid lines represent saddle-node bifurcation and Hopf bifurcation, respectively. GH and BT represent degenerate Hopf bifurcation and Bogdanov–Takens bifurcation, respectively

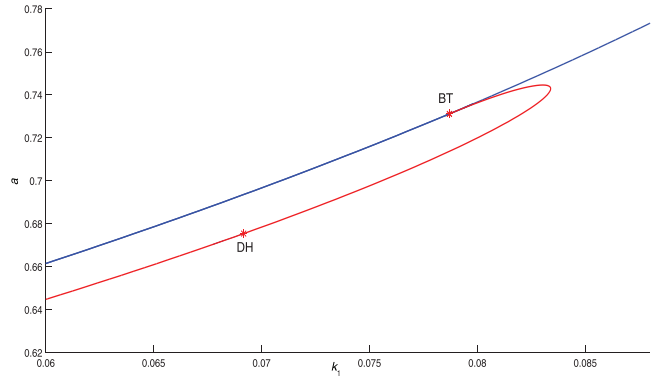


TABLE 2 Dynamical behaviors in Figure 6 with $(c, k_1, k_2) = (\frac{2}{5}, \frac{17}{250}, \frac{3}{25})$

a	Positive equilibria and types	Limit cycle and homoclinic loop
0.7	No	No (Figure 6A)
0.672	E_{11} (saddle), E_{12} (unstable focus)	No (Figure 6B)
0.67129	E_{11} (saddle), E_{12} (stable focus)	An unstable limit cycle (Figure 6C)
0.67128	E_{11} (saddle), E_{12} (stable focus)	An unstable limit cycle, a homoclinic loop (Figure 6D)
0.6712	E_{11} (saddle), E_{12} (stable focus)	Two limit cycles (the inner one unstable) (Figure 6E)
0.57	E_{11} (saddle), E_{12} (stable focus)	No (Figure 6F)

TABLE 3 Dynamical behaviors in Figure 7 with $(c, k_1, k_2) = (\frac{2}{5}, \frac{69}{1000}, \frac{3}{25})$

a	Positive equilibria and types	Limit cycle and homoclinic loop
0.7	No	No (Figure 7A)
0.678	E_{11} (saddle), E_{12} (unstable focus)	No (Figure 7B)
0.67538	E_{11} (saddle), E_{12} (unstable focus)	A homoclinic loop (Figure 7C)
0.675	E_{11} (saddle), E_{12} (unstable focus)	A stable limit cycle (Figure 7D)
0.674846	E_{11} (saddle), E_{12} (stable focus)	Two limit cycle (the inner one unstable) (Figure 7E)
0.67	E_{11} (saddle), E_{12} (stable focus)	No (Figure 7F)

Next, we carry out numerical simulation with the help of MATLAB software. Fix $(c, k_2) = (\frac{2}{5}, \frac{3}{20})$ in system (6), and using the program MATCONT, we get the two-parameter bifurcation diagram in (k_1, a) -plane as shown in Figure 5. While we cannot numerically plot homoclinic bifurcation curve HO and saddle-node bifurcation curve DC of limit cycles, we will give evidences to show that they indeed exist in Figure 5. The phase portraits are given in Figures 6, 7, and 8, where parameter values and corresponding dynamical behaviors are given in Tables 2, 3, and 4, respectively. The parameters values in Figures 6, 7, and 8 are taken from three parallel lines $k_1 = \frac{34}{500}, k_1 = \frac{69}{1000}$, and $k_1 = \frac{3}{40}$ in Figure 5, respectively.

- (1) From Figure 6 and Table 2, as a decrease, system (6) undergoes successively: saddle-node bifurcation, subcritical Hopf bifurcation, attracting homoclinic bifurcation, and saddle-node bifurcation of limit cycles;

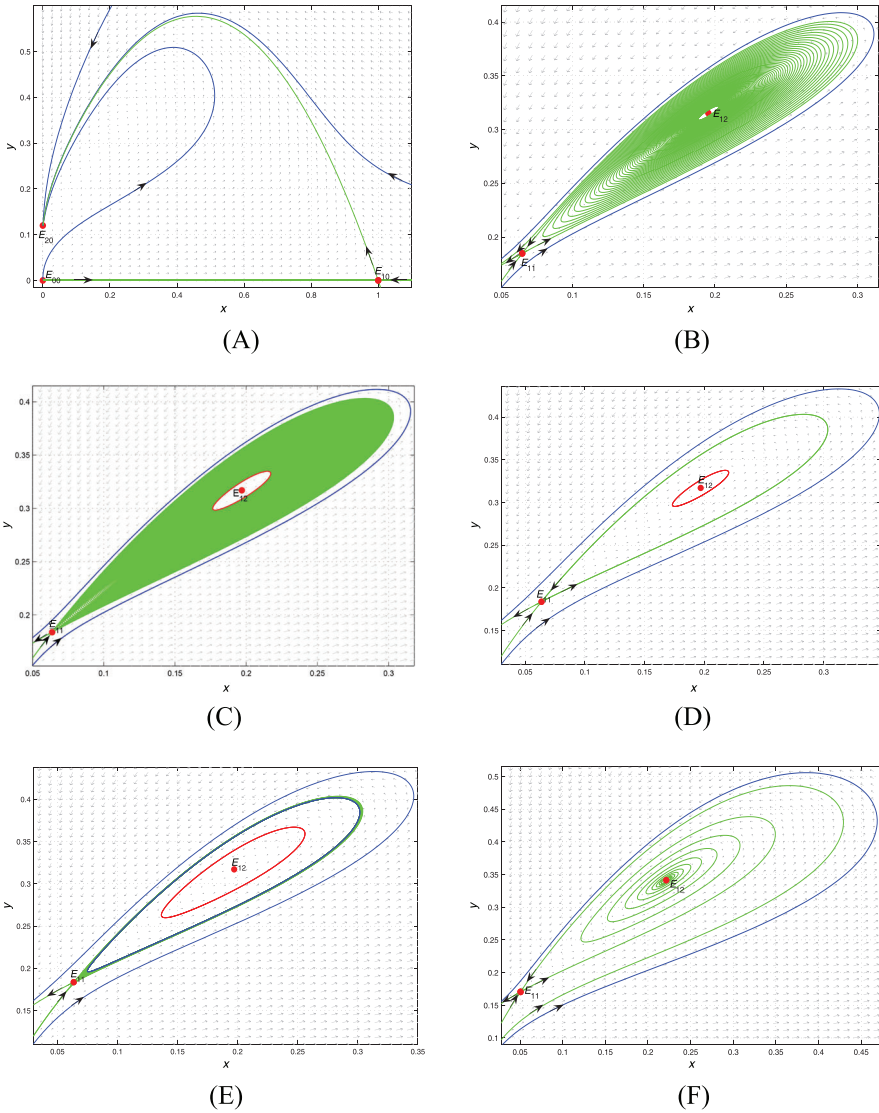


FIGURE 6 Phase portraits of system (6) with $(c, k_1, k_2) = (\frac{2}{5}, \frac{17}{250}, \frac{3}{25})$. (A) $a = 0.7$, (B) $a = 0.672$, (C) $a = 0.67129$, (D) $a = 0.67128$, (E) $a = 0.6712$, (F) $a = 0.57$. The detailed dynamical behaviors are described in Table 2

TABLE 4 Dynamics behaviors in Figure 8 with $(c, k_1, k_2) = (\frac{2}{5}, \frac{3}{40}, \frac{3}{25})$

a	Positive equilibria and types	Limit cycle and homoclinic loop
0.71	E_{11} (saddle), E_{12} (unstable focus)	No (Figure 8A)
0.7029	E_{11} (saddle), E_{12} (unstable focus)	A homoclinic loop (Figure 8B)
0.7	E_{11} (saddle), E_{12} (unstable focus)	A stable limit cycle (Figure 8C)
0.695	E_{11} (saddle), E_{12} (stable focus)	No (Figure 8D)

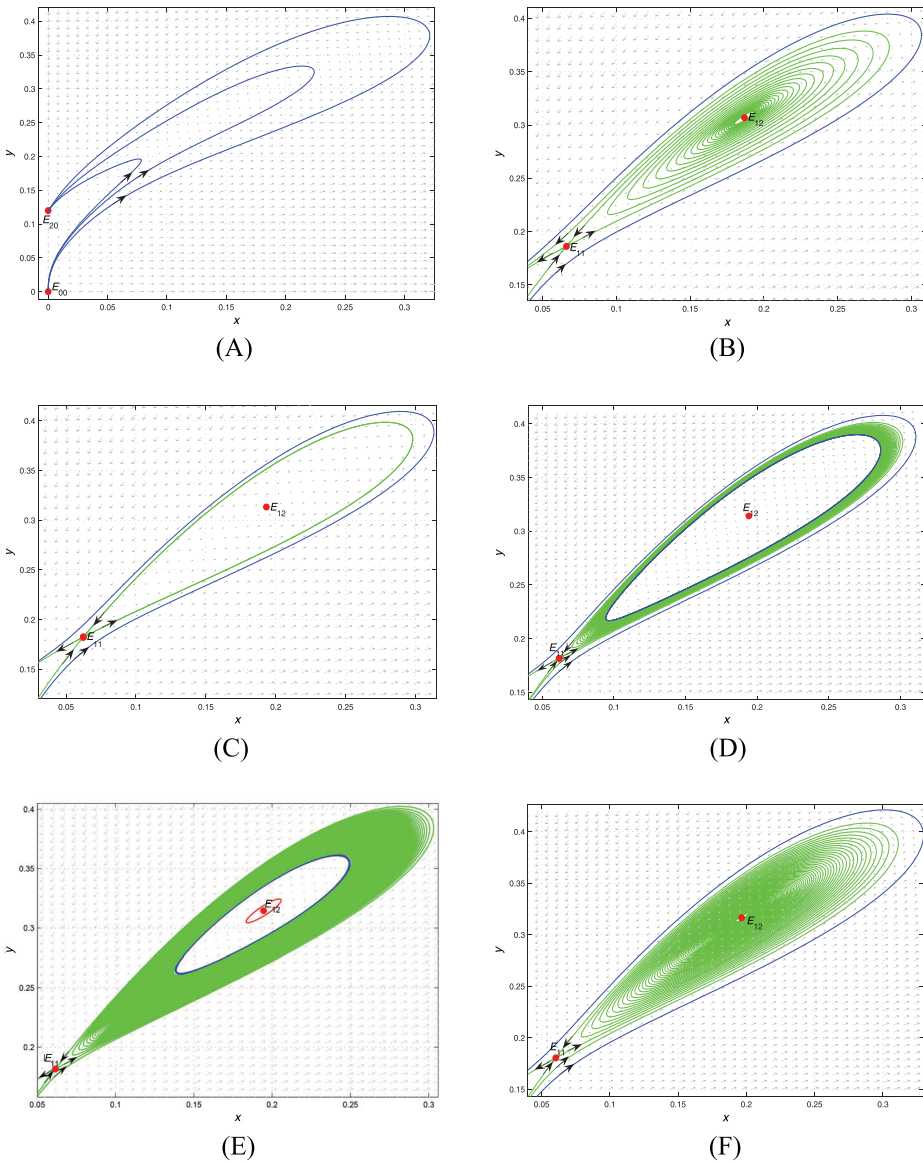


FIGURE 7 Phase portraits of system (6) with $(c, k_1, k_2) = (\frac{2}{5}, \frac{69}{1000}, \frac{3}{25})$. (A) $a = 0.7$, (B) $a = 0.678$, (C) $a = 0.7$, (D) $a = 0.695$, (E) $a = 0.674846$, (F) $a = 0.67$. The detailed dynamical behaviors are described in Table 3

- (2) From Figure 7 and Table 3, as a decrease, system (6) undergoes successively: saddle-node bifurcation, attracting homoclinic bifurcation, subcritical Hopf bifurcation, and saddle-node bifurcation of limit cycles;
- (3) From Figure 8 and Table 4, as a decrease, system (6) undergoes successively: attracting homoclinic bifurcation, supercritical Hopf bifurcation.

From the phase portraits in Figures 6, 7, and 8, we can infer that there exist two curves \mathcal{HO} and \mathcal{DC} in Figure 5.

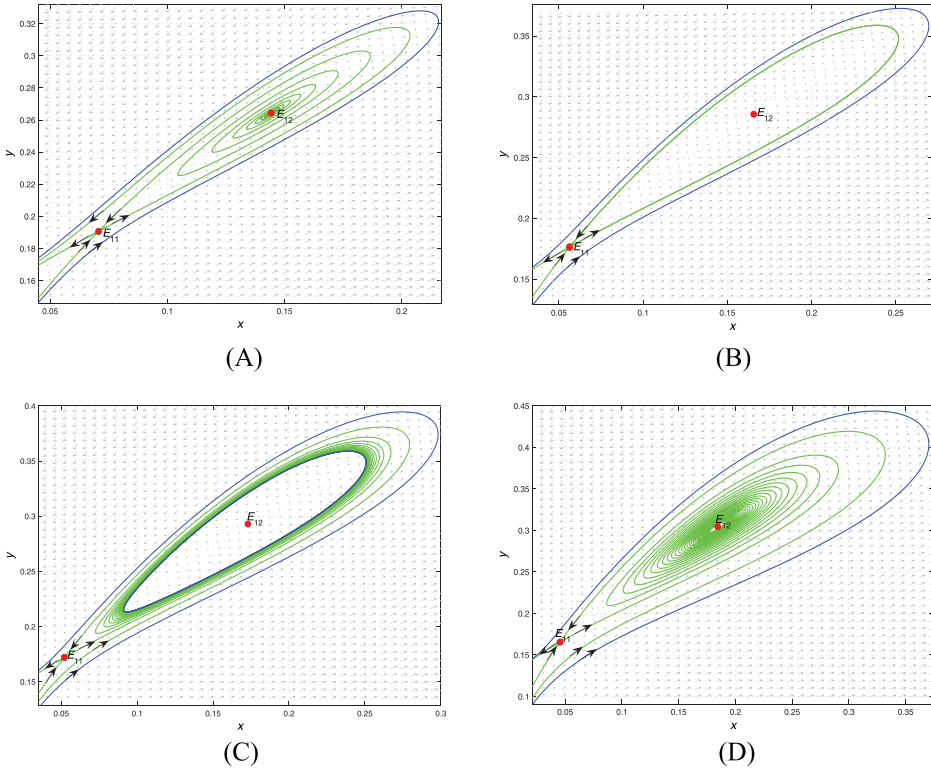


FIGURE 8 Phase portraits of system (6) with $(c, k_1, k_2) = (\frac{2}{5}, \frac{3}{40}, \frac{3}{25})$. (A) $a = 0.71$, (B) $a = 0.7029$, (C) $a = 0.671295$, (D) $a = 0.67128$. The detailed dynamical behaviors are described in Table 4

3 | CHANGING ENVIRONMENT

In this section, we study the effect of the rate of environmental change in carrying capacity on the dynamics of system (4). In detail, we first use the bifurcation software MATCONT to plot the one-parameter (or two-parameter) bifurcation diagram in $K - y$ (or $K - K_2 - y$) plane for system (3), then plot some “representative trajectories” (“time series,” which are actually the projection of the trajectories of system (4) on the $K - y$ plane) for system (4) and include them into the bifurcation diagram (see Figures 9–12). In Figures 9–11, the stable and unstable steady states for system (3) are indicated by blue solid and dashed curves, respectively. The maximum and minimum values of stable and unstable oscillations are indicated by blue filled and open circles, respectively. The “representative” trajectories (time series) for system (4) are plotted by red solid curves.

3.1 | One environmental variable

In system (4), the carrying capacity $K(t)$ increases with time when $\mu > 0$, and decreases when $\mu < 0$. According to the bifurcations and dynamics of system (3) given in Section 2, we classify the effect of μ in system (4) as the following three cases:

Case (I): Monostability (a stable state or a stable oscillation). When system (3) exhibits supercritical Hopf bifurcation around the unique positive equilibrium $E_{12}(x_{12}, y_{12})$, system (3) can

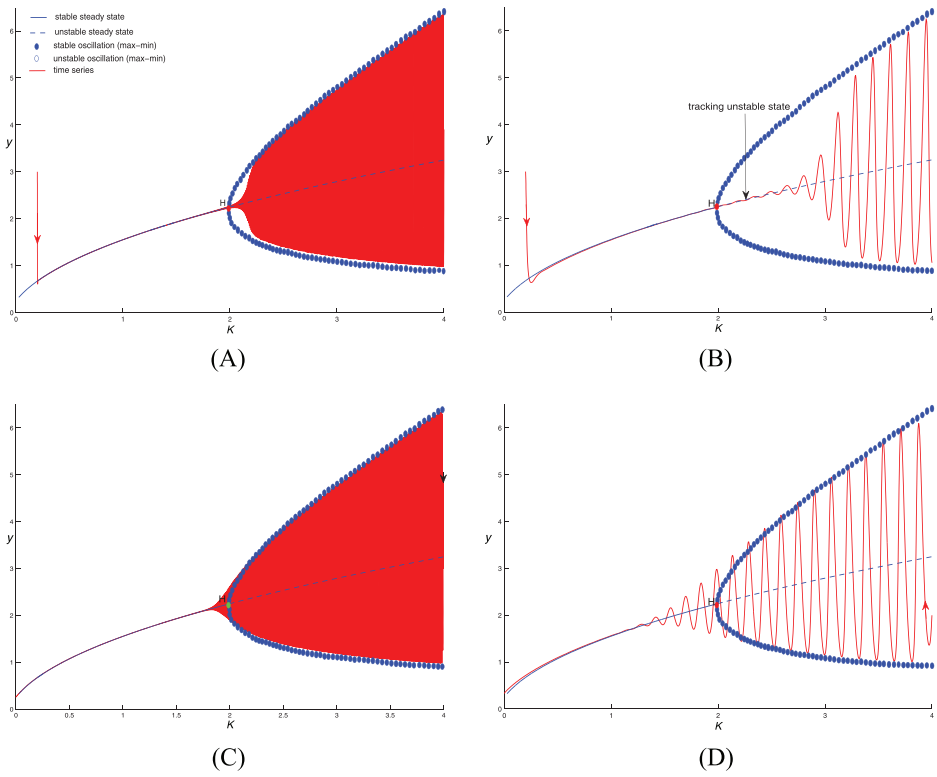


FIGURE 9 Dynamics in model (4) for different rate of environmental change μ : (A) $\mu = 0.0002$, (B) $\mu = 0.0038$, where the red time series track unstable state E_{12} at the Hopf bifurcation (H), (C) $\mu = -0.0002$, (D) $\mu = -0.0038$. All equilibria are represented in blue color curves, whereas time series in temporally varying environment is represented by red color curves. Other parameters are $r = 0.5$, $s = 0.125$, $m = 0.125$, $n = 0.25$, $h = 4$, and $K_2 = 0.25$

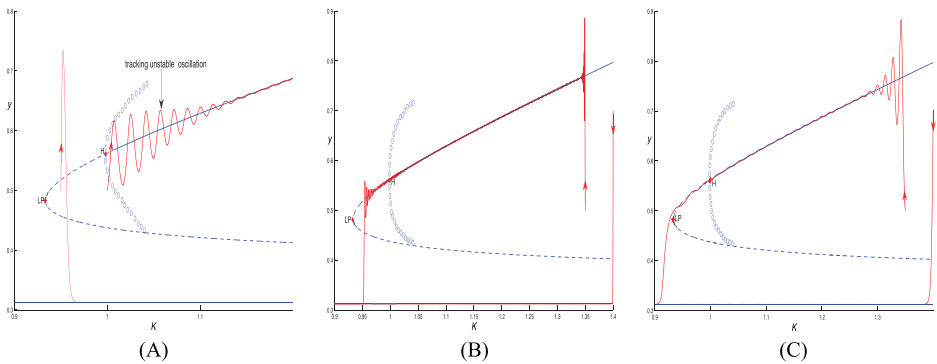


FIGURE 10 Dynamics in model (4) for different rate of environmental change μ : (A) $\mu = 0.0005$, (B) $\mu = -0.0005$, (C) $\mu = -0.005$. The time series track an unstable oscillation at the Hopf bifurcation point (H) When $\mu = 0.0005$. Other parameters are $r = 1$, $s = 0.25$, $m = 0.5$, $n = 0.125$, $h = 1$, and $K_2 = 0.3125$

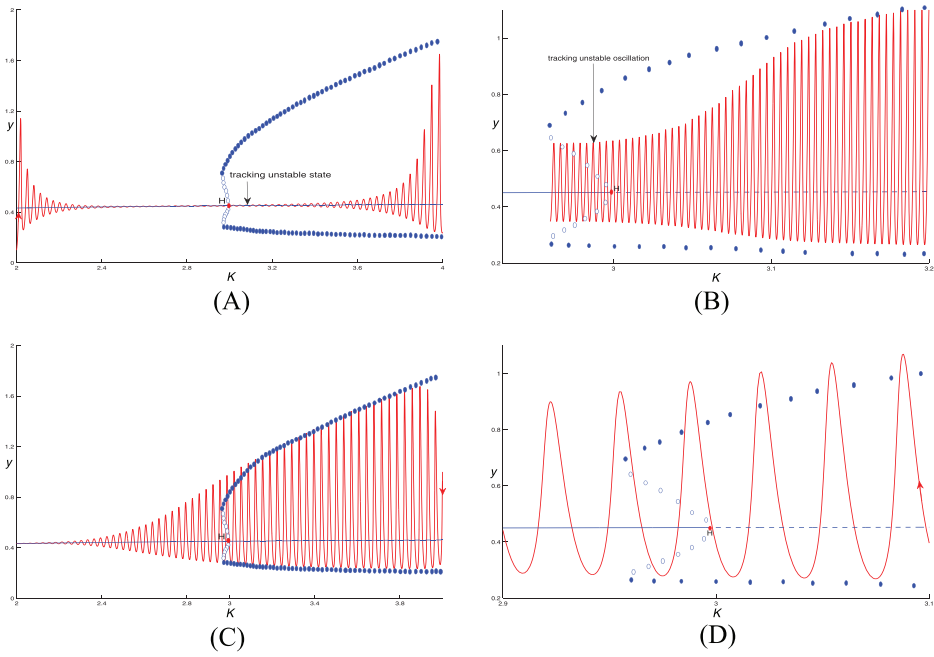


FIGURE 11 Dynamics in model (4) for different rate of environmental change μ : (A) $\mu = 0.005$, (B) $\mu = 0.0002$, (C-D) $\mu = -0.005$. Other parameters are $r = 1$, $s = 0.25$, $m = 1$, $n = 0.325$, $h = 2$, and $K_2 = 0.15125$

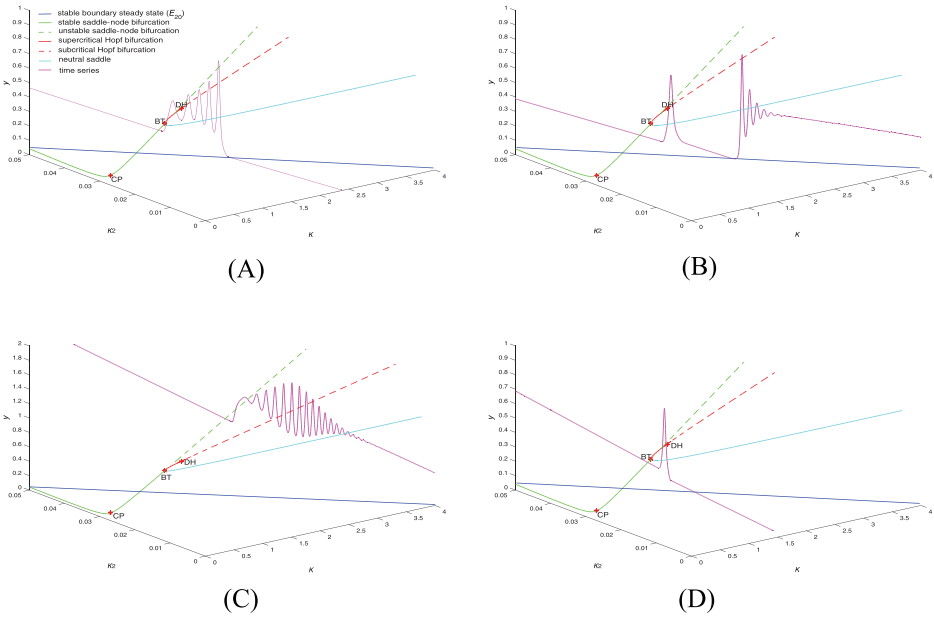


FIGURE 12 Rate-dependent dynamics in system (81): changing carrying capacity over time with a rate (A) $\mu = 0.001$, $\mu_1 = 0.0001$; (B) $\mu = 0.001$, $\mu_1 = -0.0001$; (C) $\mu = -0.001$, $\mu_1 = -0.0001$; (D) $\mu = 0.001$, $\mu_1 = 0.0001$. All equilibria are represented in blue color curves, whereas time series in temporally varying environment is represented by red color curves. Other parameters are $r = 1$, $s = 0.7$, $m = \frac{9(\sqrt{257}-1)}{160}$, $n = 0.025$, $h = 1$

have a stable equilibrium E_{12} or a stable limit cycle for different parameter values (see Figure 9). In Figure 9A,B, the carrying capacity $K(t)$ increases since $\mu > 0$, we can see that the predator population $y(t)$ of system (4) (in red curve), starting along a stable state E_{12} of system (3), can first track the unstable state E_{12} when the system crosses supercritical Hopf bifurcation point (H), and then tend to a stable oscillation (limit cycle) of system (3). Thus, this tracking, leading to transient dynamics, can be used to predict regime shifts (from a positive stable state to a stable coexistent oscillation). Moreover, we find that if the rate of environmental change is higher, then the system (4) tracks the unstable state E_{12} longer to the stable oscillation. In Figure 9C,D, the carrying capacity $K(t)$ decreases since $\mu < 0$, it can be seen that the predator population $y(t)$ of system (4), for lower rate of environmental change, lasts longer before it switches from tracking the stable oscillation to the stable state E_{12} .

Case (II): Bistability (two stable states). When system (3) exhibits subcritical Hopf bifurcation around the positive equilibrium $E_{12}(x_{12}, y_{12})$, system (3) can have two stable equilibria: E_{12} , $E_{20}(0, k_2)$ and an unstable limit cycle simultaneously (see Figure 10). From Figure 10A, we can see that the predator population $y(t)$ of system (4) (in red curve), either tends to the predator-only stable state E_{20} of system (3), or track the unstable oscillation when the system crosses subcritical Hopf bifurcation point (H) and finally tends to the positive stable state E_{12} . Thus, it is clear that the initial values are important to the persistence and coexistence of both populations due to multiple attractors and regime shifts. From Figure 10B–C, it can be seen that the predator population $y(t)$ of system (4), for lower rate of environmental change, lasts longer before it switches from the positive stable state E_{12} to the predator-only stable state E_{20} .

Case (III): Bistability (a stable state and a stable oscillation). When system (3) exhibits subcritical Hopf bifurcation around the unique positive equilibrium $E_{12}(x_{12}, y_{12})$, system (3) can have a stable equilibria: E_{12} , a stable limit cycle and an unstable limit cycle simultaneously (see Figure 11). From Figure 11A, we can see that the predator population $y(t)$ of system (4) (in red curve) track the unstable state E_{12} when the system crosses subcritical Hopf bifurcation point (H) and finally tends to the stable oscillation. From Figure 11B, we can see that the predator population $y(t)$ track the small unstable oscillation after subcritical Hopf bifurcation point (H) and finally tends to the big stable oscillation. From Figure 11C–D, it can be seen that the predator population $y(t)$ of system (4) undergoes the regime shifts (from a stable coexistent oscillation to a positive stable state).

3.2 | Two environmental variables

Here, we consider two environmental variables $K(t) = \mu t + K_0$ and $K_2(t) = \mu_1 t + K_{20}$, that is, the following system:

$$\begin{aligned} \dot{x} &= rx \left(1 - \frac{x}{K} \right) - \frac{mxy}{n+x}, \\ \dot{y} &= sy \left(1 - \frac{y}{hx + K_2} \right), \\ \dot{K} &= \mu, \\ \dot{K}_2 &= \mu_1. \end{aligned} \tag{81}$$

Following the same logic, we first use the bifurcation software MATCONT to plot the two-parameter bifurcation diagram in $K - K_2 - y$ plane for system (3), then plot some “representative” trajectories (time series) for system (81) and include them into the bifurcation diagram (see Figure 12). In Figure 12, system (3) can undergo degenerate Hopf bifurcation of codimension 2, in which there exists tristability (two stable equilibria E_{20}, E_{12} and a stable limit cycle). Thus system (81) can exhibit multiple regime shifts depending on different parameter values and different initial values.

3.3 | Periodic environmental variable

In this subsection, we consider a periodic environment by choosing $K(t) = K_0 + \gamma \sin(2\pi t)$ for seasonality, then system (4) becomes

$$\begin{aligned}\dot{x} &= rx \left(1 - \frac{x}{K}\right) - \frac{mxy}{n+x}, \\ \dot{y} &= sy \left(1 - \frac{y}{hx + K_2}\right), \\ \dot{K} &= 2\pi\gamma \cos(2\pi t),\end{aligned}\tag{82}$$

where $0 < \gamma < K_0$. The carrying capacity reaches a maximum value $K_0 + \gamma$ at time $t = \frac{1}{4} + i$, and a minimum value $K_0 - \gamma$ when $t = \frac{3}{4} + i$, where i is an integer (representing the i th year).

We rewrite system (82) as

$$\dot{Y} = f(Y) + \gamma g_1(t, Y),\tag{83}$$

where $Y = (x, y)^T$, $f(Y) = (rx(1 - \frac{x}{K_0}) - \frac{mxy}{n+x}, sy(1 - \frac{y}{hx+K_2}))^T$, $g_1(t, Y) = (\frac{rx^2}{K_0^2} \sin(2\pi t) + O(\gamma), 0)^T$.

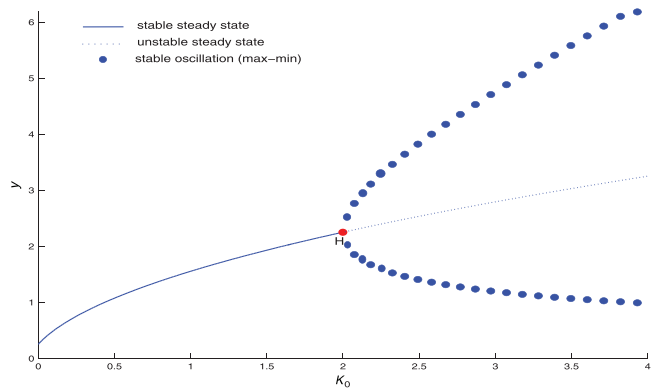
Define

$$\begin{aligned}K^H &= \frac{rx_1(n+2x_1)}{(r-s)x_1 - ns}, \quad m^H = \frac{(r+s)(n+x_1)^2}{(n+2x_1)(hx_1+K_2)}, \quad d_1 = \frac{(nr+(r-s)x_1)hx_1 - s(n+2x_1)K_2}{(n+2x_1)(K_2+hx_1)}, \\ \sigma_1^0 &= \frac{(r+s)\sigma_{11}}{8sh(n+x_1)(n+2x_1)^2(K_2+hx_1)^2(K_2s(n+2x_1) - hx_1(nr+(r-s)x_1))},\end{aligned}\tag{84}$$

where σ_1^0 is the first Lyapunov coefficient of system (83)| $_{\gamma=0}$ (i.e., system (3) with $K = K_0$) around the positive equilibrium $E_1(x_1, y_1)$ and

$$\begin{aligned}\sigma_{11} &= 2hr(r-s)(3hn - 2K_2)x_1^4 + (2hnK_2(r^2 + s^2) + h^2n^2(4r^2 - 11rs + s^2) - 2(r-s)^2K_2^2)x_1^3 \\ &\quad + n(hnK_2(2r^2 - 3rs + 9s^2) + 2(r-3s)sK_2^2 - 7rsn^2h^2)x_1^2 - sn^2(rn^2h^2 + nhK_2(r-6s) \\ &\quad + (r+3s)K_2^2)x_1 + hK_2s^2n^4.\end{aligned}\tag{85}$$

FIGURE 13 Bifurcation diagram in $K_0 - y$ plane of system (83) $_{|\gamma=0}$ with $r = 0.5, s = 0.125, m = 0.125, n = 0.25, h = 4, K_2 = 0.25$ and initial value $(x_0, y_0) = (0.4, 1.99)$



Based on Lemma 2, we have the following results about system (83) $_{|\gamma=0}$ (i.e., system (3) with $K = K_0$).

Lemma 5. *If $0 < K_2 < \frac{rn}{m}$, then system (83) $_{|\gamma=0}$ (i.e., system 3 with $K = K_0$) has a unique positive equilibrium $E_1(x_1, y_1)$. Moreover,*

- (i) *if $0 < K_0 < K^H$ and $r > \frac{n+x_1}{x_1}s$, or $r \leq \frac{n+x_1}{x_1}s$, then E_1 is a hyperbolic stable focus (or node);*
- (ii) *if $K_0 = K^H$ and $r > \frac{n+x_1}{x_1}s$, then E_1 is a center-type equilibrium;*
- (iii) *if $K_0 > K^H$, then E_1 is a hyperbolic unstable focus (or node).*

Remark 2. Let $r = 0.5, s = 0.125, m = 0.125, n = 0.25, h = 4$, and $K_2 = 0.25$. The bifurcation diagram in $K_0 - y$ plane for system (83) $_{|\gamma=0}$ is given in Figure 13, from which we can see that E_1 is hyperbolic and stable when $K_0 < 2$ and unstable when $K_0 > 2$, system (83) $_{|\gamma=0}$ undergoes a supercritical Hopf bifurcation at $K_0 = 2$, and a stable limit cycle occurs when $K_0 > 2$.

Next, we study theoretically the bifurcation of a hyperbolic stable equilibrium E_1 in system (83) $_{|\gamma=0}$ (i.e., system (3) with $K = K_0$) into an asymptotically stable periodic solution in system (83), and the bifurcation of a stable limit cycle around E_1 in system (83) $_{|\gamma=0}$ into an attracting invariant torus in system (83).⁴⁴⁻⁴⁶

According to Theorem 2 in Brauer⁴⁴ and Lemma 5(i), we have the following result about the bifurcation of a hyperbolic stable equilibrium E_1 in system (83) $_{|\gamma=0}$ into an asymptotically stable periodic solution in system (83) (or system 82).

Theorem 6. *If the conditions in Lemma 5(i) hold, then system (83) (i.e., system 82) has an asymptotically stable periodic solution $P(t, \gamma)$ of period 1 for all sufficiently small γ with $\lim_{\gamma \rightarrow 0} P(t, \gamma) = (x_1, y_1)$.*

Remark 3. Let $r = 0.5, s = 0.125, m = 0.125, n = 0.25, h = 4, K_2 = 0.25$, and $K_0 = 1.5$, the equilibrium E_1 in system (83) $_{|\gamma=0}$ is hyperbolic and stable (see Figure 13). The bifurcation diagram in $\gamma - x$ plane for system (83) is given in Figure 14. When $\gamma = 0.02$, the phase portrait, an attractor

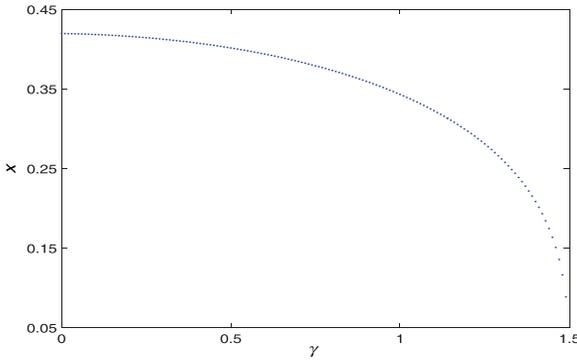


FIGURE 14 Bifurcation diagram in $\gamma - x$ plane of system (83) with $r = 0.5$, $s = 0.125$, $m = 0.125$, $n = 0.25$, $h = 4$, $K_2 = 0.25$, and initial value $(x_0, y_0, K_0) = (0.4, 1.99, 1.5)$

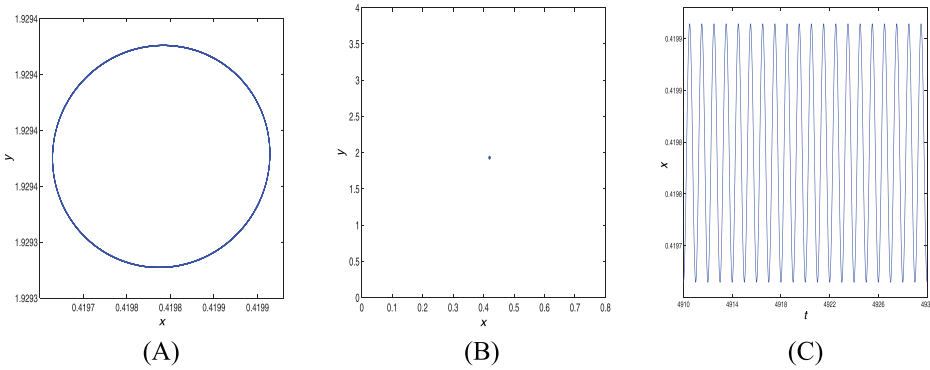


FIGURE 15 (A) The phase portrait of system (83) with $\gamma = 0.02$ in Figure 14. (B) An attractor of the Poincaré map corresponding to (A). (C) The time series of the prey corresponding to (A)

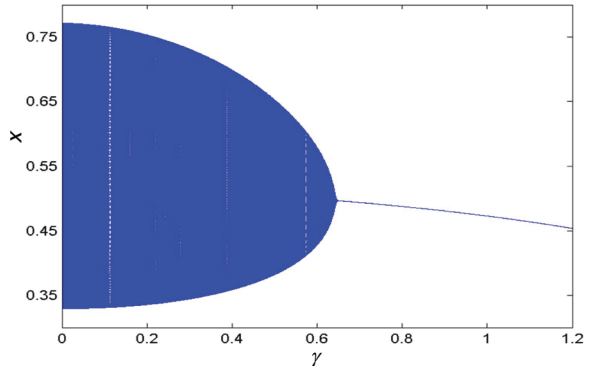
of the Poincaré map and the time series of the prey for system (83) are given in Figure 15, where E_1 becomes as an asymptotically stable 1-periodic solution.

Combining the generic Hopf bifurcation theorem and Theorem 6.3 in Chow et al,⁴⁶ we have the following results about the bifurcation of a stable limit cycle around E_1 in system (83)_{| $\gamma=0$} (i.e., system 3 with $K = K_0$) into an attracting invariant torus in system (83).

Theorem 7. *If $m = m^H$, $\sigma_1^0 < 0$, and the conditions in Lemma 5(ii) hold, then there exist neighborhoods U of $(K_0, \gamma) = (K^H, 0)$, W of $E_1(x_1, y_1)$ and a C^p ($p \geq 3$) submanifold C of U of codimension one such that $U \setminus C = U_1 \cup U_2$ can be classified as two open disjoint sets and the following conclusions hold:*

- (i) *if $(K_0, \gamma) \in U_1$, then there exists a unique one-periodic solution $\varphi(\lambda)$ of (83) in W , which is asymptotically stable.*
- (ii) *if $(K_0, \gamma) \in U_2$, then there exist a one-periodic solution $\varphi(\lambda)$ of (83) in W and an invariant torus S_λ of (83) in $\mathbb{R} \times W$. Furthermore, $\varphi(\lambda)$ is unstable and S_λ is asymptotically stable.*

FIGURE 16 Bifurcation diagram in $\gamma - x$ plane of system (83) with $r = 0.5, s = 0.125, m = 0.125, n = 0.25, h = 4, K_2 = 0.25,$ and initial value $(x_0, y_0, K_0) = (0.4, 1.99, 2.1)$



Proof. We need to check the following three nonresonant conditions (according to the notations in Theorem 6.3 in Chow et al⁴⁶):

$$\begin{aligned} \beta_0 &< 0, \\ \text{Det}(e^{BT} - I) &\neq 0, \\ m + n \frac{2\pi}{T} &\neq 0, \quad 0 < |m| + |n| \leq 4, \quad m, n \text{ are integers,} \end{aligned} \tag{86}$$

where β_0 is the first Lyapunov coefficient σ_1^0 for the center-type equilibrium E_1 , and $T = 1$ is the period of perturbed terms in system (83); $B = \begin{pmatrix} 0 & \sqrt{d_1} \\ -\sqrt{d_1} & 0 \end{pmatrix}$, $d_1 > 0$ is given in (84) and I is the identical matrix. It is obvious that these three conditions are satisfied if the conditions in this theorem hold. Hence, according to Theorem 6.3 in Section 12 of Chow et al,⁴⁶ the results hold. ■

Remark 4. Let $r = 0.5, s = 0.125, m = 0.125, n = 0.25, h = 4, K_2 = 0.25, K_0 = 2.1,$ and initial value $(x_0, y_0) = (0.4, 1.99)$, system $(83)|_{\gamma=0}$ has a stable limit cycle around E_1 (see Figure 13). The bifurcation diagram in $\gamma - x$ plane for system (83) is given in Figure 16. When $\gamma = 0.6$, the phase portrait, an attractor of the Poincaré map and the time series of the prey for system (83) are given in Figure 17, we can see that a stable limit cycle around E_1 in system $(83)|_{\gamma=0}$ becomes as an attracting invariant torus in system (83). When $\gamma = 0.8$, the attracting invariant torus becomes as an asymptotically stable one-period periodic solution (see Figure 18).

Finally, based on the above theoretical analysis and numerical simulations, we have the following conclusions about the effects of a periodic environment in system (83) on the dynamics of system $(83)|_{\gamma=0}$:

- (i) When the initial carrying capacity $K_0 = 1.5 < K_H = 2$, a hyperbolic stable equilibrium E_1 in system $(83)|_{\gamma=0}$ (i.e., system 3 with $K = K_0$) will bifurcate into an asymptotically stable periodic solution in system (83) (or system 82). The trajectory of system (83) will eventually converges to a stable periodic solution (see Figures 13, 14, and 15).
- (ii) When the initial carrying capacity $K_0 = 2.1 > K_H = 2$, a stable limit cycle around E_1 in system $(83)|_{\gamma=0}$ (i.e., system 3 with $K = K_0$) will bifurcate into an attracting invariant torus in

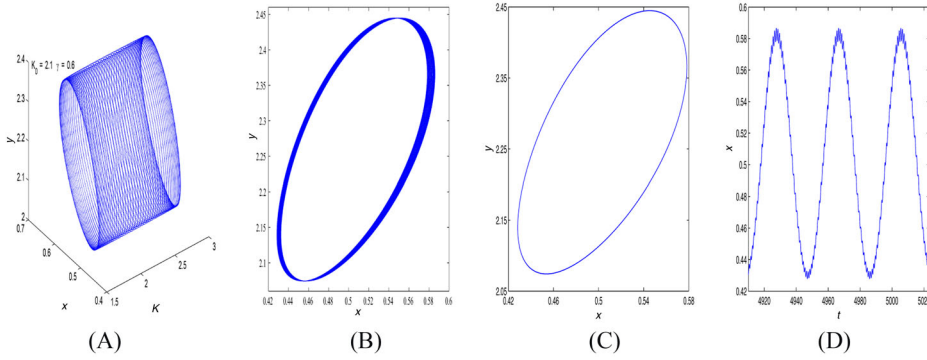


FIGURE 17 (A) Phase portrait for $\gamma = 0.6$ in Figure 16. (B) Projection of phase portrait corresponding to (A). (C) An attractor of the Poincaré map. (D) The time series of the prey

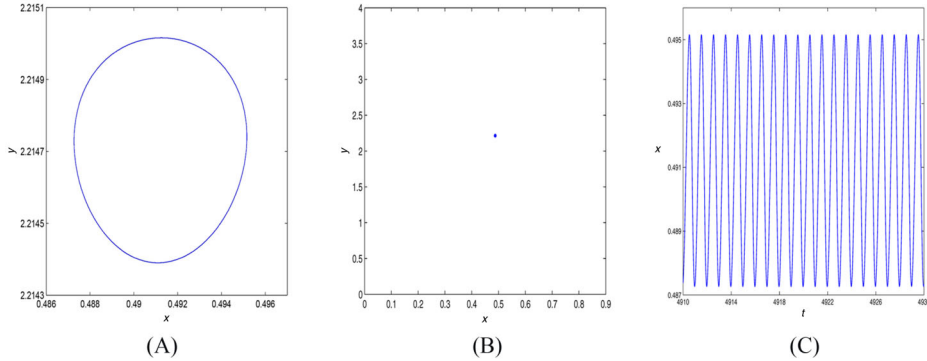


FIGURE 18 (A) Phase portrait for $\gamma = 0.8$ in Figure 16. (B) An attractor of the Poincaré map corresponding to (A). (C) The time series of the prey corresponding to (A)

system (83). The trajectory of system (82) will eventually converge to a stable invariant torus for small periodic amplitude (see Figures 13, 16, and 17) and to a stable periodic solution for large periodic amplitude (see Figures 13, 16, and 18).

4 | DISCUSSION

We studied the impact of environmental change on the modified Holling–Tanner model, where the predator is the so-called generalist who has alternative food sources by adding an extra constant carrying capacity K_2 for the predator.

In a constant environment $\mu = 0$, model (4) becomes model (3) that always has three boundary equilibria and at most two positive equilibria. When there exists a unique and elementary positive equilibrium, there were extensive studies about the qualitative behaviours, such as the global stability and the existence of limit cycle, and so forth. However, the bifurcations with high codimension still remain open. In this paper, we have shown that the highest codimension for a nilpotent cusp is 3, and the model can undergo degenerate Bogdanov–Takens bifurcation of codimension 3. Moreover, when the model has a center-type equilibrium, we have shown that it is

a weak focus of order at most 2, and the model can exhibit Hopf bifurcation of codimension 2. Thus, we can infer that the cusp of codimension 3 is the organizing center of the bifurcation set. On the other hand, we have shown the existence of two limit cycles enclosing E_{12} in Figure 2E–F, which means that the unique positive equilibrium E_{12} is not globally asymptotically stable when it is locally asymptotically stable. Finally, numerical simulations, including bifurcation diagram and corresponding phase portraits, the coexistence of a limit cycle and a homoclinic cycle, two limit cycles enclosing a stable equilibrium, are presented to illustrate the theoretical results.

The generalist predator in (3) can cause richer dynamical behaviors and bifurcation phenomena. Compared modified Holling–Tanner model (3) with Holling–Tanner model (2), we can see that model (2) has a unique boundary equilibrium and at most one positive equilibrium, while model (3) has three boundary equilibria and at most two positive equilibria. Moreover, there exists only Hopf bifurcation in (2), while in (3) we have shown not only the existence of Hopf bifurcation with codimension up to 2, but also a degenerate Bogdanov–Takens bifurcation of codimension 3, which includes a series of bifurcations with lower codimension, such as codimension 1: saddle-node bifurcation, Hopf bifurcation, homoclinic bifurcation, and saddle-node bifurcation of limit cycles; codimension 2: Bogdanov–Takens bifurcation, degenerate Hopf bifurcation, degenerate homoclinic bifurcation, and Hopf and homoclinic bifurcations simultaneously. It is worth noting that there exists tristability phenomenon in Figure 2E–F for model (3), that is, two stable equilibria E_{20}, E_{12} and a stable limit cycle, which cannot occur in model (2).

The generalist predator in (3) can also cause the extinction of prey for all positive initial densities under some conditions. For Holling–Tanner model (2) with specialist predator, both predator and prey populations with positive initial values will persist forever for model (2).^{12,13} While for modified Holling–Tanner model (3) with generalist predator, from Remark 1, we can see that there exists a threshold K_2^* for K_2 (an extra constant carrying capacity coming from other food sources for predators) such that if $K_2 > K_2^*$, then the prey will tend to extinction and predators always persist for all positive initial populations.

In the real world, predator–prey systems are much more complex than what a two-dimensional model can capture. It will be interesting and challenging to consider the following problems: (i) the effect of generalist predation on both the prey and predators, that is, add a directly density-dependent mortality to the prey's equation and suppose that the predator's equation is logistic or logistic-like form in the absence of the prey; (ii) consider multiple preys and a generalist predator species in a high-dimensional model; (iii) consider the spatial effect on predator–prey systems with generalist predator, especially the effect on the tristability or two coexisting periodic oscillations in system (3).

In a changing environment, our study links the transient dynamics to rigorous bifurcation results for asymptotic dynamics. Possible regime shifts are visualized to illustrate the pivotal role of unstable states. How long the solution under environmental change stays near an unstable state depends on the rate of climate change. This work can be helpful in understanding the resilience and restoration of ecological systems under continuous climate change. More empirical and theoretical studies need to be accumulated for capturing the underlying mechanisms in more realistic, complex ecological interactions.

ACKNOWLEDGMENTS

Research was partially supported by the National Natural Science Foundation of China (NSFC) (No. 11871235) and the Natural Sciences and Engineering Research Council of Canada (NSERC) (RGPIN-2020-03911 and RGPAS-2020-00090).

ORCID

Hao Wang  <https://orcid.org/0000-0002-4132-6109>

REFERENCES

1. Freedman HI, Mathsen RM. Persistence in predator-prey systems with ratio-dependent predator influence. *Bull Math Biol.* 1993;55:817-827.
2. Hsu SB, Huang TW. Global stability for a class of predator-prey system. *SIAM J Appl Math.* 1995;55:763-783.
3. Freedman HI. *Deterministic Mathematical Models in Population Ecology.* Marcel Dekker; 1980.
4. Gause GF. *The Struggle for Existence.* Williams and Wilkins; 1934.
5. Leslie PH. Some further notes on the use of matrices in population mathematics. *Biometrika.* 1948;35:213-245.
6. May RM. *Stability and Complexity in Model Ecosystems.* Princeton University Press; 1973.
7. Leslie PH, Gower JC. The properties of a stochastic model for the predator-prey type of interaction between two species. *Biometrika.* 1960;47:219-234.
8. Tanner JT. The stability and the intrinsic growth rates of prey and predator populations. *Ecology.* 1975;56:855-867.
9. Collings JB. The effects of the functional response on the bifurcation behavior of a mite predator-prey interaction model. *J Math Biol.* 1997;36:149-168.
10. Hsu SB, Huang TW. Uniqueness of limit cycles for a predator-prey system of Holling and Leslie type. *Can Appl Math Q.* 1998;6:91-117.
11. Hsu SB, Huang TW. Hopf bifurcation analysis for a predator-prey system of Holling and Leslie type. *Taiwan J Math.* 1999;3:35-53.
12. Gasull A, Kooij RE, Torregrosa J. Limit cycles in the Holling-Tanner model. *Publ Mat.* 1997;41:149-167.
13. Sáez E, González-Olivares E. Dynamics of a predator-prey model. *SIAM J Appl Math.* 1999;59:1867-1878.
14. Braza PA. The bifurcation structure of the Holling-Tanner model for predator-prey interactions using two-timing. *SIAM J Appl Math.* 2003;63:889-904.
15. Liang Z, Pan H. Qualitative analysis of a ratio-dependent Holling-Tanner model. *J Math Anal Appl.* 2007;334:954-964.
16. Huang J, Ruan S, Song J. Bifurcations in a predator-prey system of Leslie type with generalized Holling type III functional response. *J Differ Equ.* 2014;257:1721-1752.
17. Dai Y, Zhao Y, Sang B. Four limit cycles in a predator-prey system of Leslie type with generalized Holling type III functional response. *Nonlinear Anal Real World Appl.* 2019;50:218-239.
18. Wang C, Zhang X. Relaxation oscillations in a slow-fast modified Leslie-Gower model. *Appl Math Lett.* 2019;87:147-153.
19. Li Y, Xiao D. Bifurcations of a predator-prey system of Holling and Leslie types. *Chaos Solitons Fractals.* 2007;34:606-620.
20. Huang J, Xia X, Zhang X, Ruan S. Bifurcation of codimension 3 in a predator-prey system of Leslie type with simplified Holling type IV functional response. *Int J Bifurcat Chaos.* 2016;26:1650034(11).
21. Zhang J, Su J. Bifurcations in a predator-prey model of Leslie-type with simplified Holling type IV functional response. *Int J Bifurcat Chaos.* 2021;31:2150054(17).
22. Holling CS. The functional response of invertebrate predators to prey density. *Mem Entomol Soc Can.* 1965;45:3-60.
23. Hanski I, Hansson L, Henttonen H. Specialist predators, generalist predators and the microtine rodent cycle. *J Anim Ecol.* 1991;60:353-367.
24. Erbach A, Lutscher F, Seo G. Bistability and limit cycles in generalist predator-prey dynamics. *Ecol Complex.* 2013;14:48-55.
25. Lindström T. Qualitative analysis of a predator-prey system with limit cycles. *J Math Biol.* 1993;31:541-561.
26. Xiao D, Zhang KF. Multiple bifurcations of a predator-prey system. *Discrete Continuous Dyn Syst Ser B.* 2007;8:417-437.
27. Magal C, Cosner C, Ruan S, Casas J. Control of invasive hosts by generalist parasitoids. *Math Med Biol.* 2008;25:1-20.
28. Xiang C, Huang J, Ruan S, Xiao D. Bifurcation analysis in a host-generalist parasitoid model with Holling II functional response. *J Differ Equ.* 2020;268:4618-4662.

29. Yuan P, Chen L, You M, Zhu H. Dynamics complexity of generalist predatory mite and the leafhopper pest in tea plantations. *J Dyn Differ Equ*. 2021. <https://doi.org/10.1007/s10884-021-10079-1>.
30. van Leeuwen E, Jansen VAA, Bright PW. How population dynamics shape the functional response in a one-predator-two-prey system. *Ecology*. 2007;88:1571-1581.
31. Aziz-Alaoui MA, Daher Okiye M. Boundedness and global stability for a predator-prey model with modified Leslie-Gower and Holling-type II schemes. *Appl Math Lett*. 2003;16:1069-1075.
32. Zhu Y, Wang K. Existence and global attractivity of positive periodic solutions for a predator-prey model with modified Leslie-Gower Holling-type II schemes. *J Math Anal Appl*. 2011;384(2):400-408.
33. Li X, Song J. Global stability of a predator-prey model with modified Leslie-Gower and Holling-type schemes. Preprint.
34. Giné J, Valls C. Nonlinear oscillations in the modified Leslie-Gower model. *Nonlinear Anal Real World Appl*. 2020;51:103010.
35. Arumugam R, Lutscher F, Guichard F. Tracking unstable states: ecosystem dynamics in a changing world. *OIKOS*. 2021;130(4):525-540. <https://doi.org/10.1111/oik.08051>
36. Gelfand I, Kapranov M, Zelevinsky A. *Discriminants, Resultants and Multidimensional Determinants*. Birkhäuser; 1994.
37. Yang L. Recent advances on determining the number of real roots of parametric polynomials. *J Symb Comput*. 1999;28:225-242.
38. Zhang Z, Ding T, Huang W, Dong Z. *Qualitative Theory of Differential Equations*. Translations of Mathematical Monographs. Vol. 101. American Mathematical Society; 1992.
39. Huang J, Gong Y, Ruan S. Bifurcation analysis in a predator-prey model with constant-yield predator harvesting. *Discrete Continuous Dyn Syst Ser B*. 2013;18:2101-2121.
40. Lamontagne Y, Coutu C, Rousseau C. Bifurcation analysis of a predator-prey system with generalized Holling type III functional response. *J Dyn Differ Equ*. 2008;20:535-571.
41. Dumortier F, Roussarie R, Sotomayor J. Generic 3-parameter families of vector fields on the plane, unfolding a singularity with nilpotent linear part. The cusp case of codimension 3. *Ergod Theory Dyn Syst*. 1987;7:375-413.
42. Li C, Li J, Ma Z. Codimension 3 B-T bifurcation in an epidemic model with a nonlinear incidence. *Discrete Continuous Dyn Syst Ser B*. 2015;20:1107-1116.
43. Huang J, Liu S, Ruan S, Zhang X. Bogdanov-Takens bifurcation of codimension 3 in a predator-prey model with constant-yield predator harvesting. *Commun Pur Appl Anal*. 2016;15:1041-1055.
44. Brauer F. Periodic solutions of some ecological models. *J Theor Biol*. 1977;69:143-152.
45. Chen J, Huang J, Ruan S, Wang J. Bifurcations of invariant tori in predator-prey models with seasonal prey harvesting. *SIAM J Appl Math*. 2013;73:1876-1905.
46. Chow SN, Hale JK. *Methods of Bifurcation Theory*. Springer-Verlag; 1982.

How to cite this article: Xiang C, Huang J, Wang H. Linking bifurcation analysis of Holling–Tanner model with generalist predator to a changing environment. *Stud Appl Math*. 2022;1–40. <https://doi.org/10.1111/sapm.12492>

APPENDIX A: COEFFICIENTS IN THE PROOF OF THEOREM 2

$$\begin{aligned} \check{a}_{10} = \check{b}_{10} = c, \quad \check{a}_{01} = \check{b}_{01} = -c, \quad \check{a}_{20} = \frac{a^2 - (1-a)c - c^2}{a(1-a)}, \quad \check{a}_{11} = \frac{c^2 - a^2}{a(1-a)}, \quad \check{a}_{30} = \frac{(1+c)(c^2 - a^2)}{a^2(1-a)^2}, \\ \check{a}_{21} = \frac{(a-c)(a+c)^2}{a^2(1-a)^2}, \quad \check{a}_{40} = \frac{(a-c)(1+c)(a+c)^2}{a^3(1-a)^3}, \quad \check{a}_{31} = \frac{(c-a)(a+c)^3}{a^3(1-a)^3}, \\ \check{b}_{20} = -\frac{c(a+c)^2}{a(1-a)(1+c)}, \quad \check{b}_{11} = \frac{2c(a+c)^2}{a(1-a)(1+c)}, \quad \check{b}_{02} = -\frac{c(a+c)^2}{a(1-a)(1+c)}, \end{aligned}$$

$$\begin{aligned}
\check{b}_{30} &= \frac{c(a+c)^4}{a^2(1-a)^2(1+c)^2}, & \check{b}_{21} &= -\frac{2c(a+c)^4}{a^2(1-a)^2(1+c)^2}, & \check{b}_{12} &= \frac{c(a+c)^4}{a^2(1-a)^2(1+c)^2}, \\
\check{b}_{40} &= -\frac{c(a+c)^6}{a^3(1-a)^3(1+c)^3}, & \check{b}_{31} &= \frac{2c(a+c)^6}{a^3(1-a)^3(1+c)^3}, & \check{b}_{22} &= -\frac{c(a+c)^6}{a^3(1-a)^3(1+c)^3}, \\
\check{c}_1 &= -\frac{c^2}{a}, & \check{c}_2 &= \frac{a^2(-2c+1)-2ac^2+c^2}{ac(a-1)(c+1)}, & \check{c}_3 &= \frac{c(a^2-c^2)}{(a-1)a^2}, \\
\check{c}_4 &= -\frac{(a+c)(a^2c-a^2+4ac^2+2ac+2a-c^3-5c^2-2c)}{a^2(c+1)(a-1)^2}, \\
\check{c}_5 &= -\frac{(a+c)^3(a(3c^2+3c+1)-c(c^2+3c+1))}{a^2c^2(a-1)^2(c+1)^2}, & \check{c}_6 &= \frac{c(a+c)^2(a-c^2)}{a^3(c+1)(a-1)^2}, \\
\check{c}_7 &= -\frac{(a+c)^2(2a^3c+a^2(3c^2-4c-1)+2a(2c^3+c^2+3c+1)-c(c^3+6c^2+5c+2))}{a^3(a-1)^3(c+1)^2}, \\
\check{c}_8 &= -\frac{(a+c)^3(a^3(4c^3+6c^2+4c+1)+a^2(4c+1)c^3+a(c^2-3c-1)c^3-c^3(c^3+4c^2+3c+1))}{a^3c^3(a-1)^3(c+1)^3}. \quad (\text{A1})
\end{aligned}$$

APPENDIX B: THE COEFFICIENTS IN (47) AND (65), f_2 IN (48)

$$\begin{aligned}
\hat{C}_{11} &= \frac{(1+a-z)(c+z)}{z(1-z)^2}, & \hat{C}_{02} &= \frac{(c+z)\sqrt{c(1-z)(az-c(1-a-z))}}{cz(1-z)^2}, & \hat{C}_{21} &= \frac{a(c+z)^2}{z^2(1-z)^3}, \\
\hat{C}_{12} &= \frac{a(c+z)^2\sqrt{c(1-z)(az-c(1-a-z))}}{cz^2(1-z)^4}, & \hat{D}_{20} &= -\frac{cC_{111}+zC_{112}+ac^2(a+z-1)}{(z-1)^2z(c(a+z-1)+az)}, \\
\hat{D}_{11} &= -\frac{c^2C_{113}-cC_{114}+zC_{115}}{z(z-1)^2\sqrt{c(1-z)(c(a+z-1)+az)}}, \\
\hat{D}_{02} &= \frac{c^2(a+z-1)+(a-4)cz+3cz^2+c+(z-1)z^2}{c(z-1)^2z}, \\
\hat{D}_{30} &= -\frac{(c+z)(a^2(c+z)+a(c(2z-1)+z^2)+z(z-1)^2)}{(z-1)^2z^2(c(a+z-1)+az)}, \\
\hat{D}_{21} &= -\frac{(c+z)(2a^2(c+z)+a(c^2+c(7z-3)+3z^2)+3z(z-1)^2)}{(z-1)^2z^2\sqrt{c(1-z)(c(1-a-z)-az)}}, \\
\hat{D}_{12} &= \frac{(c+z)(a^2(c+z)+a(c^2+c(7z-3)+3z^2)+3z(z-1)^2)}{c(z-1)^3z^2}, \\
\hat{D}_{03} &= -\frac{(c+z)\sqrt{c(1-z)(c(1-a-z)-az)}(a(c(2z-1)+z^2)+z(z-1)^2)}{c^2z^2(1-z)^4}, \\
\hat{D}_{40} &= -\frac{a(c+z)^2}{(z-1)^2z^2(c(a+z-1)+az)}, & \hat{D}_{04} &= -\frac{a(c+z)^2(c(a+z-1)+az)}{c^2z^2(1-z)^4}, \\
\hat{D}_{31} &= -\frac{4a(c+z)^2}{(z-1)^2z^2\sqrt{c(1-z)(c(1-a-z)-az)}},
\end{aligned}$$

$$\hat{D}_{22} = \frac{6a(c+z)^2}{c(z-1)^3z^2}, \quad \hat{D}_{13} = -\frac{4a(c+z)^2\sqrt{c(1-z)(c(1-a-z)-az)}}{c^2z^2(1-z)^4},$$

$$C_{111} = 2a^2z + a(2z^2 - 3z + 1) + (2z - 1)(z - 1)^2, \quad C_{112} = a^2z + a(z - 1)^2 + z(z - 1)^2,$$

$$C_{113} = a^2 + a(z - 1) + (z - 1)^2, \quad C_{114} = -(2a^2z + a(2z^2 - 3z + 1) + (5z - 2)(z - 1)^2),$$

$$C_{115} = a^2z + a(z - 1)^2 + 2z(z - 1)^2. \tag{B1}$$

$$A_{00} = \frac{a^*c(a^* - 1)(c + 1)(\eta_2(a^* + c) + (a^* - 1)\eta_1)}{(a^* + c)^2((a^* - 1)a^* - \eta_2(a^* + c))}, \quad A_{01} = \frac{c(a^* - 1)(a^* + \eta_1)}{\eta_2(a^* + c) - (a^* - 1)a^*},$$

$$A_{10} = 1 + \frac{c(a^* - 1)}{a^* + c} - \frac{(a^* - 1)a^*(c + 1)(a^* + \eta_1)}{(a^* + c)((a^* - 1)a^* - \eta_2(a^* + c))} + A_1,$$

$$A_{20} = \frac{(a^* - 1)^2a^*c(c + 1)(a^* + \eta_1)}{((a^* - 1)a^* - \eta_2(a^* + c))^3} - \frac{(a^* - 1)a^*(c + 1)(a^* + \eta_1)}{((a^* - 1)a^* - \eta_2(a^* + c))^2} - 1,$$

$$A_{11} = \frac{(a^* + c)(a^* + \eta_1)(a^{*2} - a^*c - a^*\eta_2 - a^* - c\eta_2 + c)}{(a^{*2} - a^*\eta_2 - a^* - c\eta_2)^2},$$

$$A_{30} = -\frac{(a^* - 1)a^*(c + 1)(a^* + c)(a^* + \eta_1)(a^{*2} - a^*c - a^*\eta_2 - a^* - c\eta_2 + c)}{(a^{*2} - a^*\eta_2 - a^* - c\eta_2)^4},$$

$$A_{21} = \frac{(a^* + c)^2(a^* + \eta_1)(a^{*2} - a^*c - a^*\eta_2 - a^* - c\eta_2 + c)}{(a^{*2} - a^*\eta_2 - a^* - c\eta_2^3)},$$

$$A_{40} = -\frac{(a^* - 1)a^*(c + 1)(a^* + c)^2(a^* + \eta_1)(a^{*2} - a^*c - a^*\eta_2 - a^* - c\eta_2 + c)}{(a^{*2} - a^*\eta_2 - a^* - c\eta_2)^5},$$

$$A_{31} = \frac{(a^* + c)^3(a^* + \eta_1)(a^{*2} - a^*c - a^*\eta_2 - a^* - c\eta_2 + c)}{(a^{*2} - a^*\eta_2 - a^* - c\eta_2)^4},$$

$$B_{00} = \frac{(a^* - 1)a^*c(c + 1)\eta_3}{(a^* - 1)a^*(c + 1) - \eta_3(a^* + c)^2}, \quad B_{10} = \frac{(a^* - 1)^2a^{*2}c(c + 1)^2}{((a^* - 1)a^*(c + 1) - \eta_3(a^* + c)^2)^2},$$

$$B_{01} = \frac{c\eta_3(a^* + c)^2 + (a^* - 1)a^*(c + 1)}{\eta_3(a^* + c)^2 - (a^* - 1)a^*(c + 1)}, \quad B_{20} = \frac{(a^* - 1)^2a^{*2}c(c + 1)^2(a^* + c)^2}{((a^* - 1)a^*(c + 1) - \eta_3(a^* + c)^2)^3},$$

$$B_{11} = -\frac{2(a^* - 1)a^*c(c + 1)(a^* + c)^2}{((a^* - 1)a^*(c + 1) - \eta_3(a^* + c)^2)^2}, \quad B_{02} = -\frac{c(a^* + c)^2}{\eta_3(a^* + c)^2 - (a^* - 1)a^*(c + 1)},$$

$$B_{30} = \frac{(a^* - 1)^2a^{*2}c(c + 1)^2(a^* + c)^4}{((a^* - 1)a^*(c + 1) - \eta_3(a^* + c)^2)^4}, \quad B_{21} = -\frac{2(a^* - 1)a^*c(c + 1)(a^* + c)^4}{((a^* - 1)a^*(c + 1) - \eta_3(a^* + c)^2)^3},$$

$$B_{12} = \frac{c(a^* + c)^4}{((a^* - 1)a^*(c + 1) - \eta_3(a^* + c)^2)^2}, \quad B_{40} = \frac{(a^* - 1)^2a^{*2}c(c + 1)^2(a^* + c)^6}{((a^* - 1)a^*(c + 1) - \eta_3(a^* + c)^2)^5},$$

$$\begin{aligned}
 B_{31} &= -\frac{2(a^* - 1)a^*c(c + 1)(a^* + c)^6}{((a^* - 1)a^*(c + 1) - \eta_3(a^* + c)^2)^4}, & B_{22} &= \frac{c(a^* + c)^6}{((a^* - 1)a^*(c + 1) - \eta_3(a^* + c)^2)^3}, \\
 A_1 &= \frac{(a^* - 1)c((a^* + c)((a^* - 1)a^{*2} + \eta_2^2(a^* + c) - 2(a^* - 1)a^*\eta_2) + (a^* - 1)a^*(c + 1)\eta_1)}{(a^* + c)((a^* - 1)a^* - \eta_2(a^* + c))^2}.
 \end{aligned}
 \tag{B2}$$

$$\begin{aligned}
 f_2 &= 3c(c + z)^6(c^2 + 4cz - c + 2z^2)a^7 + c(1 - z)(c + z)^5(79c^3 + 291c^2z - 70c^2 + 68cz^2 + 51cz - 9c \\
 &\quad - 40z^3 + 8z^2)a^6 - c(1 - z)^2(c + z)^4(488c^4 + 2390c^3z - 575c^3 + 3105c^2z^2 - 994c^2z + 84c^2 \\
 &\quad + 1688cz^3 - 449cz^2 - 42cz + 3c + 294z^4 + 46z^3 - 8z^2)a^5 + (1 - z)^3(c + z)^3(1137c^6 + 6780c^5z \\
 &\quad - 1681c^5 + 13803c^4z^2 - 5750c^4z + 603c^4 + 13658c^3z^3 - 6570c^3z^2 + 883c^3z - 59c^3 + 7452c^2z^4 \\
 &\quad - 3380c^2z^3 + 425c^2z^2 + 9c^2z + 2192cz^5 - 612cz^4 - 50cz^3 + 6cz^2 + 248z^6)a^4 - (1354c^7 \\
 &\quad + 9513c^6z - 2482c^6 + 25205c^5z^2 - 11899c^5z + 1395c^5 + 33726c^4z^3 - 20174c^4z^2 + 3817c^4z \\
 &\quad - 267c^4 + 25772c^3z^4 - 16304c^3z^3 + 3274c^3z^2 - 189c^3z + 11926c^2z^5 - 7214c^2z^4 + 1340c^2z^3 \\
 &\quad - 127c^2z^2 + 3420cz^6 - 1994cz^5 + 272cz^4 + 496z^7 - 248z^6)(1 - z)^4(c + z)^2a^3 + (872c^9 + 8024c^8z \\
 &\quad - 1997c^8 + 30071c^7z^2 - 13931c^7z + 1542c^7 + 59801c^6z^3 - 37491c^6z^2 + 7226c^6z - 417c^6 \\
 &\quad + 69027c^5z^4 - 50729c^5z^3 + 12063c^5z^2 - 967c^5z + 47097c^4z^5 - 37922c^4z^4 + 9601c^4z^3 - 895c^4z^2 \\
 &\quad + 17594c^3z^6 - 15814c^3z^5 + 3707c^3z^4 - 345c^3z^3 + 2062c^2z^7 - 3294c^2z^6 + 485c^2z^5 - 828cz^8 \\
 &\quad - 230cz^7 - 248z^9)(1 - z)^5a^2 + c(1 - z)^6(-285c^8 - 2764c^7z + 838c^7 - 10358c^6z^2 + 5892c^6z \\
 &\quad - 837c^6 - 18696c^5z^3 + 14592c^5z^2 - 3656c^5z + 284c^5 - 16301c^4z^4 + 15472c^4z^3 - 4690c^4z^2 \\
 &\quad + 496c^4z - 4956c^3z^5 + 6970c^3z^4 - 2264c^3z^3 + 284c^3z^2 + 2068c^2z^6 + 668c^2z^5 - 177c^2z^4 + 1840cz^7 \\
 &\quad - 152cz^6 + 372z^8)a + 36c^2(1 - z)^7(c^7 + 11c^6z - 4c^6 + 41c^5z^2 - 28c^5z + 5c^5 + 59c^4z^3 - 58c^4z^2 \\
 &\quad + 19c^4z - 2c^4 + 16c^3z^4 - 30c^3z^3 + 13c^3z^2 - 2c^3z - 28c^2z^5 + 8c^2z^4 - c^2z^3 - 20cz^6 + 4cz^5 - 4z^7)
 \end{aligned}
 \tag{B3}$$